DEUTSCHES ELEKTRONEN-SYNCHROTRON DESY

DESY 75/17
July 1975

Some Recent Results on Photoproduction and Electroproduction of Hadrons

by

G. Weber
Deutsches Elektronen-Synchrotron DESY, Hamburg
and
II. Institut für Experimentalphysik der Universität Hamburg

2 HAMBURG 52 · NOTKESTIEG 1

To be sure that your preprints are promptly included in the
HIGH ENERGY PHYSICS INDEX ,
send them to the following address (if possible by air mail) :

SOME RECENT RESULTS ON PHOTOPRODUCTION AND ELECTROPRODUCTION OF HADRONS

G. Weber*
Deutsches Elektronen-Synchrotron DESY, Hamburg and
II. Institut für Experimentalphysik der Universität Hamburg, Hamburg

INTRODUCTION

Given the limited time allocated to this session, I shall not try to review the whole field of electro- and photoproduction. Instead I will restrict myself to the contributions submitted to the conference and to some important developments of the past two years. My report, which can be grouped into three sections, covers the following topics:

A. Photo- and Electroproduction of π- and η-Mesons
A1. Photoproduction in the Resonance Region
A2. Electroproduction in the Resonance Region
A3. Axial Form Factor of the Nucleon
A4. Pion Form Factor
A5. Electroproduction of Neutral Pions.

B. Vector Meson Production and Compton Scattering with Real Photons
B1. Photoproduction of ρ's
B2. Photoproduction of ω's
B3. Photoproduction of Φ's
B4. Photoproduction of Higher Vector Mesons
B5. Small Angle Compton Scattering on Nuclei

C. Hadronic Final States in Electro- and Muonproduction
C1. Electroproduction of Vector Mesons
C2. Multihadronproduction by Virtual Photons.

A. Photo- and Electroproduction of π- and η-Mesons

A 1. Photoproduction in the Resonance Region

We are concerned with the reactions

1a) $\gamma p \rightarrow \pi^+ n$
1b) $\gamma p \rightarrow \pi^o p$
1c) $\gamma n \rightarrow \pi^- p$
1d) $\gamma n \rightarrow \pi^o n$

There has been a considerable improvement in the quality of data during the past two years. To give you an idea of how the photoproduction data have changed, let us have a look at Fig.1, which shows the experimental cross section[1] for backward π^+ production as measured till 1973. There is a lot of scatter of the points for a given energy region, and it is obvious that some of the errors have been underestimated. Fig.2 shows the same

*Rapporteur Talk given at the EPS International Conference on High Energy Physics Palermo, Italy, 23.-28. June, 1975

quantity measured[2] in 1975. The scatter has been strongly reduced. It is this replacement of medium accurate data by more systematic (in angle and energy) and highly accurate measurements, that is needed for multipole analysis. Fig.3, which has been prepared by G. Knies, shows the number of available data points on cross sections and polarisation parameters. Cross section data are quite abundant, whereas there is a shortage of measurements on polarisation parameters. Regarding the latter, within the past 18 months measurements in Berkeley[4], NINA[7] and Tokyo[6] have considerably increased the amount of data. We also note the first measurement of reaction Id) by a group from Kyoto[5]. Multipole analysis have been carried out independently by 4 groups[3]. The situation will be reviewed by R. G. Moorhouse.

A 2. Electroproduction in the Resonance Region

The kinematic parameters used to describe electroproduction in the one photon approximation have already been defined in the talks of Taylor and Kötz, so I do not need to define them again. Let me just remind you of the fact, that an electron of primary energy E and scattered energy E' produces a virtual photon of energy $\nu = E - E'$ and $(\text{mass})^2 = q^2 = -Q^2 = -4EE' \sin^2 \frac{\theta}{2}$. Instead of using the structure functions W_1 and W_2, we shall express the inclusive electron scattering cross section in terms of σ_L and σ_T, the cross sections for longitudinal and transverse photons:

$$\frac{d^2\sigma}{d\Omega dE'} = \Gamma(\sigma_T + \varepsilon\sigma_L)$$

$$\Gamma = \frac{d}{2\pi^2} \frac{E'}{E} \frac{K}{q^2} \frac{1}{1-\varepsilon} = \text{flux factor} \qquad (2)$$

$$K = \frac{W^2 - M^2}{2M}$$

$$\varepsilon = \left[1 + 2\text{tg}^2 \frac{\theta}{2} \left(1 + \frac{\nu^2}{q^2}\right)\right]^{-1} = \text{polarisation parameter}$$

There have been two high statistics experiments on total cross sections. One from the DESY-Karlsruhe[8] group, one from SLAC[9]. Fig.4 shows the total cross section measurements of SLAC[9] for hydrogen and deuterium at an electron scattering angle of 4°. One notices the first, second and third resonance peaks and a slight indication of a hump near 1.95 GeV, where the photoproduction cross section shows structure due to the $F_{37}(1950)$. Apart from total cross section measurements, the experimental material[10] is in general less complete than in photoproduction and, with the exception of the first resonance, rather few data exist on particular reaction channels. Measurements at NINA and at DESY indicate structure in the $\pi^+ n$ channel for small θ and in $\pi^0 p$ channel for large θ. The π^0 channel at backward angles shows drastic variations in the region of the $F_{37}(1950)$. A recent multipole analysis by Devenish and Lyth[11] will be discussed by Moorhouse.

Before leaving the resonance region let me just mention an interesting observation made with reaction

$$\gamma_v p \to \eta p \qquad (3)$$

by groups at NINA[12], Bonn[13], and DESY[14]. Fig.5 gives the q^2 dependence of the η-production cross section at the peak of the $S_{11}(1535)$. The striking feature is the slow decrease with increasing q^2, compared to the dipole formula and to a theoretical model calculation by Ravndal[15]. The angular distributions measured in the region of the second and third resonance are flat, consistent with s-wave excitation, and the W-dependence indicates the $S_{11}(1535)$ to dominate the reaction. The form factor analysis of Devenish and Lyth[11] shows qualitative agreement with quark model expectation in that the helicity structure seems to change rapidly as a function of q^2. It is therefore very important to get an experimental separation of the longitudinal and the transverse parts of the cross section. An experiment aiming at these quantities is in progress at DESY.

Since there have been very few measurements on σ_L and σ_T for single pion production, it is worth mentioning the result of a recent experiment on electroproduction of π^+ carried out at the 0.6 GeV linac at Saclay[17]. In this experiment the scattered electron and the produced π^+ were detected in coincidence, using two magnetic spectrometers. To separate σ_L and σ_T the cross section was measured for the same W and q^2 at two different polarisation parameters ε. The kinematic parameters and the results of the Saclay experiment are tabulated in Fig.6. There is a large longitudinal part, and both σ_L and σ_T have rather small errors.

A 3. Axial Form Factor of the Nucleon

There are some new results on the axial form factor $G_A(q^2)$ of the nucleon from electroproduction of charged pions in two different reactions.

The reaction

$$\gamma_v p \to \pi^+ n \qquad (4)$$

at threshold has been used in the past by several groups[18)19)20] to derive values for $G_A(q^2)$. In a contribution to this conference the DARESBURY-PISA collaboration[21] reports on the reanalysis of a previous measurement, which brings their results into better agreement with those of other groups and with the neutrino experiment. Fig.7 shows the results of the experiments of the FRASCATI[18], DESY[19] and DARESBURY-PISA[21] groups. There is now good agreement between the results of different laboratories.

Another result, using the reaction

$$\gamma_v p \to \pi^- \Delta^{++} \qquad (5)$$

was reported by the DESY-GLASGOW collaboration[23]. Strictly speaking this latter reaction does not yield the elastic axial form factor $G_A(q^2)$ of the nucleon, but the transition form factor $G_A^*(q^2)$ from the nucleon ground state to the Δ-resonance. However, we do not expect the difference between $G_A(q^2)$ and $G_A^*(q^2)$ to be very important, since the electromagnetic transition form factor $G_M^*(q^2)$ of the proton for the excitation of the Δ-resonance does not differ very much from the elastic form factor[10)22] of the proton in the range of $q^2 < 1$ GeV^2 (we expect a difference of the order of 10%). Fig.7, in which also the values derived from reaction 5) have been plotted, shows them to be in good agreement with those derived from π^+ production. The curves represent dipole expressions for

three different mass parameters. A least square fit to all points, including the π^- results, yields a mass parameter $m_A = 1.11 \pm 0.04$. The neutrino value[24] is $m_A = 0.95 \pm 0.12$ GeV. Thus the results of the pion electroproduction experiments are in excellent agreement with PCAC and current algebra.

A 4. Electroproduction of π^+ and the Pion Form Factor

Extensive measurements have been carried out by the Cornell-Harvard[25] group on the reaction 4) at high energy for q^2 up to 4 GeV^2, and analyzed in terms of the pion form factor $F_\pi(q^2)$. Fig.8a gives the values derived for $F_\pi(q^2)$ assuming the pion electroproduction amplitude to be purely isovector (V). In Fig.8b an isoscalar contribution (I) given by the experimentally determined[25] ratio

$$R = \frac{\sigma(\gamma_v d \to \pi^- p p_s)}{\sigma(\gamma_v d \to \pi^+ n n_s)} = \left|\frac{V - I}{V + I}\right|^2 \qquad (6)$$

(where the index s refers to "spectator") was assumed. Both procedures confirm, that the pion form factor is approximately given by the ρ-propagator $F_\rho(q^2)$ or by the Dirac isovector form factor $F_1^v(q^2)$, but not by the charge form factor $G_E^p(q^2)$ of the proton[22].

A 5. Electroproduction of Neutral Pions

Contrary to electroproduction of charged pions, where the one pion exchange graph can give rise to a rather large longitudinal cross section, the longitudinal cross section is expected to be small in electroproduction of neutral pions. Therefore, one might hope to get some direct information on the q^2 dependence of the transverse cross section from a comparison of photo- and electroproduction of π^0's . As already reported by Dr. Kötz, the reaction

$$\gamma_v p \to \pi^0 p \qquad (8)$$

has recently been studied at DESY[26] for an energy W of 2.55 GeV. In this experiment the geometry was chosen such as to maximize the contributions from photons polarized perpendicularly to the production plane in order to keep possible longitudinal and interference terms small. The scattered electron and the recoil proton were detected simultaneously with the decay γ rays of the π^0 , the electron and the proton by magnetic spectrometers, the γ rays by a lead glass hodoscope. They got a very clear definition of the reaction, practically free of any background. The results obtained for three values of q^2 are shown in Fig.9 as a function of t . The dashed line represents the photoproduction results. For small t , the cross section falls exponentially as in photoproduction with slopes between 4.2 and 3.6 GeV^{-2}. There is a drastic difference in the behaviour compared to photoproduction in that the exponential drop continues out to 0.8 GeV^2 and then levels off, rather than going through the so called dip at 0.5 GeV^2 and through a maximum near 1 GeV^2. For $|t| \approx 1$ GeV^2 the cross section changes by factor 9 in going from $q^2 = 0$ to $q^2 = 0.22$ GeV^2, and then shows rather little variation with q^2 . It is remarkable that the only variation occurs at very small q^2 , whereas at q^2 above 0.22 the cross section seems rather independent of q^2 . Other reactions such as multihadronproduction seem to

show a similar behaviour, although much less spectacular.

B. Vector Meson Production and Compton Scattering with Real Photons

B 1. Photoproduction of ρ-Mesons

Fig.10 shows the differential cross section for the reaction

$$\gamma p \to \rho p \tag{10}$$

as a function of the momentum transfer t for various values of the energy[27]. The cross section for small t is given by an exponential

$$\frac{d\sigma}{dt} = \left(\frac{d\sigma}{dt}\right)_o \exp(At) \tag{10a}$$

with the slope parameter A roughly equal to that of πp and compton scattering. It has been found, that the ρ production amplitude is close to being purely imaginary and that to a good approximation only isoscalar and natural parity exchanges occur in the t channel. The conclusion therefore is, that ρ production is a diffractive process.

B 2. Photoproduction of ω-Mesons

For lack of statistics, the available data on

$$\gamma N \to \omega N \tag{11}$$

are less precise than for ρ production. Fig.11 shows the differential cross sections for ρ, ω and ρ' (1600) production, as measured by the Tel Aviv group[28]. The curves represent exponentials, multiplied by the square of the deuteron form factor. The ω production results obtained so far, agree with the idea that main contributions come from π-exchange and from diffraction scattering.

B 3. Photoproduction of Φ-Mesons

The reaction

$$\gamma p \to \Phi p \tag{12}$$

should give us the clearest picture of the Pomeron at low energies. This follows from vector meson dominance and the unique quark composition of the phi, namely, $\lambda\bar{\lambda}$. The reaction $\Phi p \to \Phi p$ is shielded from ordinary Regge trajectories in the t-channel, by both s-channel and u-channel exoticity.

There are some interesting new results on phi photoproduction from a DESY-Karlsruhe collaboration[29]. This group has collected about 6000 events between 3 and 7 GeV using a tagged photon beam. Fig.12 shows the set-up. The tagging system had 43 energy channels each 50 MeV wide. The bremsstrahlung beam (7 mm FWHM) passed through a liquid H_2-target of 50 cm length, a hole in the trigger counters, and was stopped in a lead plug at the entrance of the magnet. Forward going particles were recorded in four proportional chambers in front and eight spark chambers in back of the magnet. Trigger counters and a threshold Cerenkov counter filled with Freon discriminated against pions and electrons. Their measurements were confined to $|t|$ less than 0.4 GeV^2. They got a clean separation

of elastic and inelastic events and they will eventually produce density matrix elements. So far, they have produced differential cross sections for elastic production, as shown in Fig.13. The new results indicate an exponential behaviour down to very small t with a slope around 5.5 GeV^{-2}. A slope of 5.5 GeV^{-2} is definitely larger than what one usually associates with this reaction. But most experiments in this field cover larger t-ranges and it now seems rather certain that $d\sigma/dt$ does not follow a simple exponential much beyond $t = 0.4$ GeV^2. The figure shows the data from other experiments at $|t| > 0.4$ GeV^2. The straight line is a fit to the large t data[30-34] only, and one sees a striking discrepancy between this fit and the new low t data. Notice that both groups of data, however, join up well in the overlap region around $t = 0.4$ GeV^2. The safest region to look for a possible Pomeron slope therefore seems $|t| < 0.4$ GeV^2. The DESY-Karlsruhe collaboration has re-analyzed the slopes of world data on phi production with this restriction in mind and has produced the data shown in Fig.14. This is a plot of the slope in phi-photoproduction against s, with the restriction $|t| < 0.4$ GeV^2. The straight line corresponds to a linear Pomeron trajectory with $\alpha'(0) = 0.22 \pm 0.27$. This result still has such large errors as to exclude a definite conclusion about shrinkage, although it is interesting to compare this with the value 0.278 ± 0.024 which has emerged from PP scattering at high energies.

B 4. Higher Vector Meson States

What is the situation with the so called $\rho'(1600)$? The broad (200 - 400 MeV) enhancement in the 4π mass distribution around 1.5 GeV observed by the SLAC-Streamer Chamber group[36] and by the SLAC-Berkeley[37] collaboration studying

$$\gamma p \to \pi^- \pi^+ \pi^- \pi^+ p \qquad (13)$$

was shown to have most likely spin and parity 1^-. The production properties resemble those for the rho: exponential t distribution with $A \approx 5$ GeV^{-2}; a decay distribution consistent with s-channel helicity conservation. Further support for this state came from an Adone measurement[38] observing a bump in $e^+e^- \to \pi^+\pi^+\pi^-\pi^-$ around 1.5 GeV. The contribution of the Tel Aviv group[28] mentioned before also reports evidence for this. Until recently it was an open question whether this enhancement in the 4π system with the quantum numbers of the photon is a resonance or not[39]. As discussed in session F1 there is now good evidence from $\pi\pi$ phase shift analysis for this peak near 1.6 GeV to be a resonance. It therefore seems to be clear that the so-called $\rho'(1600)$ is a resonance with the quantum numbers of the ρ.

How about the $\rho'(1250)$? This candidate for a higher vector meson state was found by SBT and DESY in the reaction[40)41]

$$\gamma p \to p\pi^+\pi^- + \text{neutrals}. \qquad (14)$$

The $\pi^+\pi^-$ + neutrals system shows a bump around 1250 MeV. This bump could be the B-meson or/and a new vector meson state. The decay distribution is consistent with either J^P assignment. The production features resemble again that for the ρ. Measurements of $\sigma(e^+e^- \to \pi^+\pi^-$ + neutrals) at Frascati[42] are not in contradiction with having a vector meson at 1.25 GeV. No new evidence has been reported to this conference.

B 5. Small Angle Compton Scattering

If the photon had a nuclear mean free path much larger than the nucleus, the total cross section for photons on nuclei would be proportional to the mass number A, and the cross section for Compton scattering in the forward direction would be proportional to A^2.

Experimentally a slower rise of the γA cross section has been observed[43]. This effect, called shadowing, is due to the coupling of the photon to the strongly interacting vector mesons with their short nuclear mean free paths. In a recent DESY experiment[44], this shadowing effect has been investigated in small angle compton scattering:

$$\gamma A \rightarrow \gamma A \qquad (15)$$

Targets of Be, C, Al, Ti, Cu, Ag and Au were placed in a carefully collimated and cleaned bremsstrahlung beam, photons scattered at angles between 10 an 50 mrad were converted in a thin radiator, and angles and momenta of the created e^+e^- pair were measured in a magnetic spectrometer. The measured scattering cross sections exhibit clear diffraction features (Fig.15) at the heavier elements, yielding nuclear radii consistent with the electron scattering[45] results. The forward compton cross sections obtained at photon energies of 3 and 5 GeV are shown in Fig.16, normalized to A^2 times the forward compton cross section of the proton. The errorbars indicate statistical errors, an additional normalization error of ±7% has to be applied at both energies. There is qualitative agreement with the VDM predictions represented by the two curves in that the deviation from unity increases with the photon energy. The data clearly demonstrate shadowing in the scattering of real photons.

C. Hadronic Final States in Electro- and Muoproduction

C 1. Electroproduction of Vector Mesons

Fig.17 shows a compilation of the cross sections from CORNELL[46], DESY[47] and SLAC[48] for the reaction

$$\gamma_V p \rightarrow \rho p \qquad (16)$$

as a function of q^2. The cross section decreases more rapidly with q^2 than the total virtual photon proton cross section by at least one power of q^2. The VDM prediction, $\sigma(Q^2) \sim [Q^2 + m_\rho^2]^{-2}$ is in agreement with the data (the curve includes kinematical corrections necessary when going from photo- to electroproduction). The data of the Santa Cruz-SLAC group[49] presented to this conference, normalized in the same way as those of the other groups, are also shown. Within their errors, they are not inconsistent with the other results and with the VDM prediction. New results on electroproduction of ω mesons have been reported by the Santa Cruz-SLAC group[49], which show, within the errors, the same q^2-dependence as the ρ-production data. There seems to be a constant ratio between ρ- and the ω-production cross section of about 4.5.

In connection with the notion of the shrinking photon, the t-dependence of ρ production as a function of q^2 is of prime interest[39]. Fig.18 shows the measured slope values[46-50] as a function of the variable

$$\Delta\tau = \frac{2\nu}{m_\rho^2 + Q^2} \quad ; \qquad 17)$$

the variable $\Delta\tau$ measures the time the photon can spend as a rho meson according to the uncertainty principle. For large values of $\Delta\tau$ (i.e. small Q^2) the slope appears to be independent of $\Delta\tau$, while for $\Delta\tau < 10$ GeV^2 ($\simeq$ 2fm) the slope seems to become smaller. Although a decreasing slope with decreasing $\Delta\tau$ agrees with what one expects, one has to keep in mind that the measurements include ρ-production by both transverse and longitudinal photons, while the comparison should be made for both components separately. Furthermore, in some of the experiments[46] the ρ-data include also the production of the ω mesons.

The decay distributions of ρ-mesons show that s-channel helicity conservation (SCHC) roughly holds (DESY[47], SLAC HBC[50]). Assuming SCHC one can deduce the ratio $R = \sigma_L/\sigma_T$ of ρ-mesons produced by longitudinal and transverse photons, and the phase δ between the two amplitudes. The result of a DESY-Streamer Chamber experiment and of other experiments are shown in Fig.19. Near threshold more longitudinal than transverse ρ mesons are produced. At higher energies this is reversed, $R = 0.2 - 0.3$. With increasing energy the L and T amplitudes come more and more in phase, in agreement with the expectation that both amplitudes should become diffractive at high energies.

In short, the vector meson production cross section decreases more rapidly with q^2 than the total cross section, indicating that diffractive processes become less important as q^2 increases.

C 2. Multihadron Production by Virtual Photons

Having seen the ρ production to drop much faster with q^2 than the total γp cross section, how do other channels behave with q^2 ? Let us first look at the mean number of charged particles. Fig.20 shows the charged multiplicity for 4 ranges of q^2 as a function of s. These results are from SLAC[51], CORNELL[52], DESY[47] and UCSC-SLAC[49]. The photoproduction data are given by a solid line. There is very little q^2 dependence of the multiplicity, except that the electroproduction data tend to be slightly below the photoproduction results. This difference, if it exists, seems to disappear at the higher energies. The multiplicity is roughly a linear function of $\ell n\, s$. Fig.21 shows the prong cross sections[47)49)53] for various energy bins as a function of q^2. The dashed lines represent photoproduction. Again one sees very little q^2-dependence except for a difference between $q^2 = 0$ and $q^2 \neq 0$; the electroproduced single prongs seem to be slightly above, the 3-prong slightly below the photoproduction cross section.

Summary

1) The axial form factor $G_A(q^2)$ of the nucleon, derived from electroproduction of charged pions is in good agreement with the neutrino results.

2) The pion form factor $F_\pi(q^2)$ is well approximated by the ρ-propagator $F_\rho(q^2)$ or the isovector Dirac form factor $F_1^V(q^2)$, but not by the nucleon form factor $G_E^P(q^2)$.

3) Photoproduction of ϕ meson yields a slope of the Pomeron trajectory consistent with high energy pp-scattering.

4) Shadowing observed in forward compton scattering is in qualitative agreement with the VDM prediction.

5) ρ- and ω-production by virtual photons shows a Q^2-dependence as predicted by VDM.

6) Existing data are not inconsistent with photon shrinkage, but do not prove it.

7) The Q^2-dependence of charged multiplicity and prong cross sections appears to be very small and only existent for $Q^2 < 0.3$ GeV^2.

8) The most dramatic Q^2-dependence reported so far, occurs in neutral pion production between $Q^2 = 0$ and $Q^2 = 0.22$ GeV^2.

In conclusion, some unexspected effects seem to exist in electroproduction in that some processes show a smooth q^2-dependence, whereas others exhibit a difference between $q^2 = 0$ and finite, but small q^2, and very little q^2-dependence for $q^2 \neq 0$. Since these effects could be due to the unknown longitudinal part of the cross section, experiments aiming at a separation of σ_L and σ_T, and measurements at very small q^2 are urgently needed.

ACKNOWLEDGEMENTS

In preparing this report I profited from discussions with many colleagues at DESY. The talk had to be given at very short notice and I want to express my special thanks to Drs. C. Berger, D. Cords, R. Devenish, R.A. Felst, J. Gayler, K. Heinloth, P. Joos, G. Knies, H. Meyer, W. McNeely, D. Schildknecht, I.O. Skillicorn, P. Söding and G. Wolf for their help in finding and understanding the relevant experimental material, and preparing tables and graphs. I am indepted to the DARESBURY-PISA, the DESY-GLASGOW and the DESY-KARLSRUHE Collaborations for supplying me with hitherto unpublished results.

* * *

REFERENCES

1) B. Bouquet et al., Phys.Rev.Lett. 27, 1244 (1971);
H. W. Dannhausen et al., Nucl.Phys. B61, 285 (1973)

2) H. W. Dannhausen, E. Durwen, H. M. Fischer, F. Kasper, M. Leneke, W. Niehaus, U. Schaefer, F. Takasaki; to be published

3) G. Knies, R. G. Moorhouse and H. Oberlack, LBL-2410 (1973);
W. J. Metcalfe and R. L. Walker, Nucl.Phys. B76, 253 (1974);
R.C.E. Devenish, D. H. Lyth and W. A. Rankin, Phys.Lett. 52B, 227 (1974);
R. L. Crawford, Glasgow University Preprint 1974; see also D. H. Lyth, Proceedings of the XVII International Conference on High Energy Physics, p.11-147, London, 1974

4) G. Knies, H. Oberlack, A. Rittenberg, M. Bogdanski, G. Smadja and E. E. Ronat, LBL-2671 (1974)

5) Y. Hemmi et al., Nucl.Phys. B55, 333 (1973)

6) P. Feller et al., Phys.Lett. B52, 105 (1974)

7) P.S.L. Booth et al., contribution 993 to the XVII International Conference on High Energy Physics, London 1974;
P. J. Bussey et al., contribution 997, ibid.

8) M. Köbberling et al., Nucl.Phys. B82, 201 (1974)

9) S. Stein et al., SLAC-PUB-1528 (1975)

10) A compilation of the experimental material available till April 1975 is to be found in J. Gayler, Electroproduction in the Resonance Region, Lecture presented at the VIII All Soviet Union High Energy Physics School, Erevan, April 1975;
see also Ref.11).

11) R. C. Devenish and D. H. Lyth, DESY 75/04 (1975)

12) S. Kummer et al., Phys.Rev.Lett. 30, 873 (1973)

13) U. Beck et al., Phys.Lett. B51, 103 (1974)

14) J.-C. Adler et al., Nucl.Phys. B91, 386 (1975)

15) F. Ravndal, Phys.Rev. D4, 1466 (1971)

16) R. G. Lipes, Phys.Rev. D5, 2849 (1972)

17) G. Bardin, J. Duclos, J. Julien, A. Magnon, B. Michel, and J. C. Montret, Preprint Saclay CEN

18) E. Amaldi et al., Phys.Lett. 41B, 216 (1972)

19) P. Brauel, F. W. Büsser, Th. Canzler, D. Cords, W. R. Dix, R. Felst, G. Grindhammer, W.-D. Kollmann, H. Krehbiel, J. Meyer and G. Weber, Phys.Lett. 45B, 389 (1973)

20) D. R. Botterill, D. W. Braben, R. Kikuchi, P. R. Norten, A. del Guerra, A. Giazotto, M. A. Giorgi, and A. Steffanini; Phys.Lett. 45B, 405 (1973)

21) A. del Guerra, A. Giazotto, M. A. Giorgi, A. Steffanini, D. R. Botterill, D. W. Braben, D. Clarke and P. R. Norton, private communication by M. A. Giorgi: their points, shown in Fig.7, were obtained using the model of Dombey and Read, Nucl.Phys. B60, 65 (1973); somewhat lower values are obtained by using the models of G. Furlan, N. Paver, and C. Verzegnassi, Nuovo Cimento 62A, 519 (1969) and of G. Benfatto, P. Nicolo and G. C. Rossi, Nucl.Phys. B50, 205 (1972)

22) For a review of the elastic nucleon form factors see R. Felst, DESY 73/56 (1973)

23) P. Joos et al., Phys.Lett. 52B, 481 (1974)

24) M. Derrick, Proceedings of the 6th International Symposium on Electron and Photon Interactions at High Energies, Bonn 1973, p. 353

25) C. J. Bebek, C. N. Brown, M. Herzlinger, S. Holmes, C. A. Lichtenstein, F. M. Pipkin, A. Raither, and L. K. Sisterton, Proceedings of the XVII International Conference on High Energy Physics, London 1974, p. IV-75, see also C. J. Bebek et al., Phys.Rev. D9, 1229 (1974)

26) F. W. Brasse, W. Fehrenbach, W. Flauger, J. Gayler, S. P. Goel, R. Haidan, U. Kötz, V. Korbel, D. Kreinick, J. Ludwig, J. May, M. Merkwitz, K.-M. Hesse, P. Schmüser, B. H. Wiik, contribution to this conference, to be published in Phys.Letters

27) K. C. Moffeit, Proceedings of the 6th International Symposium on Electron and Photon Interactions at High Energies, Bonn 1973, p.313

28) G. Alexander, O. Benary, J. Gandsman, D. Lissauer, A. Levy, J. Orenand, L. M. Rosenstein, contribution H1-05 to this conference; see also P. Benz et al., (Aachen-Bonn-Hamburg-Heidelberg-München Collaboration), Nucl.Phys. B79, 10 (1974) and DESY 74/11 (1974)

29) H.-J. Behrend, J. Bodenkamp, W. P. Hesse, D. C. Fries, P. Heine, H. Hirschmann, W. A. McNeely Jr., A. Markon and E. Seitz, DESY 75/05 (1975); Fig.13 and 14 include unpublished data obtained at photon energies between 3 and 5 GeV by the above authors

30) H. J. Besch, Nucl.Phys. B70, 149 (1974)

31) J. Ballam et al., Phys.Rev. D7, 3150 (1973)

32) R. L. Anderson et al., Phys.Rev.Lett. 30, 149 (1973)

33) C. Berger et al., Phys.Lett. 39B, 659 (1972)

34) R. L. Anderson et al., Phys.Rev. D1, 27 (1970)

35) V. Barteneo et al., Phys.Rev.Lett. 31, 1088 (1973), similar values were derived by A. Martin, Nucl.Phys. B77, 226 (1974) and by D.P. Roy et al., ibid., p.240

36) M. Davier et al., Nucl.Phys. B58, 31 (1973)

37) H. H. Bingham et al., Phys.Lett. 41B, 635 (1972)

38) G. Barbarino et al., Lett. Nuovo Cim. 3, 689 (1972)

39) G. Wolf, DESY 72/61 (1972)

40) J. Ballam et al., Nucl.Phys. B76, 375 (1974)

41) E. Rabe, Internal Report, DESY F1/2 (1971), (Diploma Thesis, unpublished)

42) M. Conversi et al., LNF 74/34 submitted to Phys.Letters

43) K. Gottfried, Proceedings of the 5th International Symposium on Electron and Photon Interactions at High Energies, p.222, Cornell 1971

44) L. Criegee, G. Franke, A. Giese, Th. Kahl, G. Poelz, U. Timm, W. Zimmermann, contribution H1-04 to this conference (unpublished)

45) L.B.R. Elton, Landolt-Börnstein N.S. I/2, 1 (1967)

46) L. Ahrens et al., Phys.Rev.Lett. 31, 131 (1973)

47) V. Eckardt et al., DESY 74/75 (1974). The points shown represent an updated, yet unpublished version of the same experiment, based on a larger data set

48) F. J. Dakin et al., Phys.Rev. D8, 687 (1973)

49) K. Bunnel et al., contribution H1-01 to this conference

50) J. Ballam et al., Phys.Rev. D10, 765 (1974)

51) K. C. Moffeit et al., Phys.Rev. 5D, 1603 (1972); J. Ballam, Phys. Rev. 5D, 545 (1972); H.H. Bingham et al., Phys.Rev. 8D, 1277 (1973)

52) P. H. Garbincius et al., Phys.Rev.Lett. 32, 328 (1974)

53) J. Ballam et al., Phys.Lett. 56B, 193 (1975).

FIGURE CAPTIONS

Fig.1 The backward π^+ production cross section as measured till 1973 (Ref.1)).

Fig.2 The backward π^+ production cross section as measured in 1975 (Ref.2)).

Fig.3 The number of cross section and polarisation parameter measurements used for multipole analysis by KMO (1973): Ref.3; Berkeley (73/74): Ref.4); Kyoto (73): Ref.5); Tokyo (74): Ref.6); NINA 74/75: Ref.7).

Fig.4 Electron proton and electron deuteron scattering cross sections measured at a laboratory angle of 4^o (Ref.9)).

Fig.5 The q^2-dependence of the η production cross section at W = 1.535 GeV. See Ref.15) and Ref.16) for origin of curves.

Fig.6 Kinematic parameters and results of the Saclay experiment.

Fig.7 Axial form factor of the nucleon.

Fig.8 Pion form factor of the nucleon (Fig.3 of Ref.24)).

Fig.9 The differential cross section for the reaction $\gamma_v p \to \pi^o p$ for various values of q^2 (Fig.4 of Ref.26)).

Fig.10 The differential ρ photoproduction cross section for different photon energies (Fig.21a of Ref.27)).

Fig.11 The differential cross sections for coherent photoproduction of ρ, ω and ρ'(160(in deuterium (Fig.2 of Ref.28)).

Fig.12 Experimental set-up for the ϕ production experiment (Fig.1a of Ref.29)).

Fig.13 The new results on ϕ production for $|t| < 0.4$ GeV^2, together with the results of previous experiments for $|t| \geq 0.4$ GeV^2.

Fig.14 Slope parameter in ϕ photoproduction as a function of s for $|t| < 0.4$ GeV^2.

Fig.15 Differential Compton cross section at 5 GeV for Be, C, Al, Ti, Cu, Ag and Au (Fig.4 of Ref.44)).

Fig.16 Shadowing effects in Compton scattering at 3 and 5 GeV (Fig.6 of Ref.44)).

Fig.17 The q^2 dependence of the total ρ production cross section. The solid curve gives the VDM prediction.

Fig.18 Slope parameter for photo- and electroproduction of ρ mesons; references for the photoproduction points are given in Ref.39); for the SLAC-HBC data see Ref.50).

Fig.19 Reaction $\gamma_v p \to \rho p$; density matrix element r_{00}^{04}, $R = \sigma_L/\sigma_T$ and cos δ as a function of W for $\langle Q^2 \rangle = 0.5$ GeV^2. Data are from Ref.47).

Fig.20 Mean charged multiplicity for 4 different Q^2 regions. The open circles, connected by a solid line, represent photoproduction, see Ref.51).

Fig.21 Fractional topological cross sections σ_n/σ_{tot} as a function of Q^2 measured by different groups. Circles: 1-prong; triangles: 3-prong; squares: 5-prong; open symbols and dashed lines represent photoproduction.

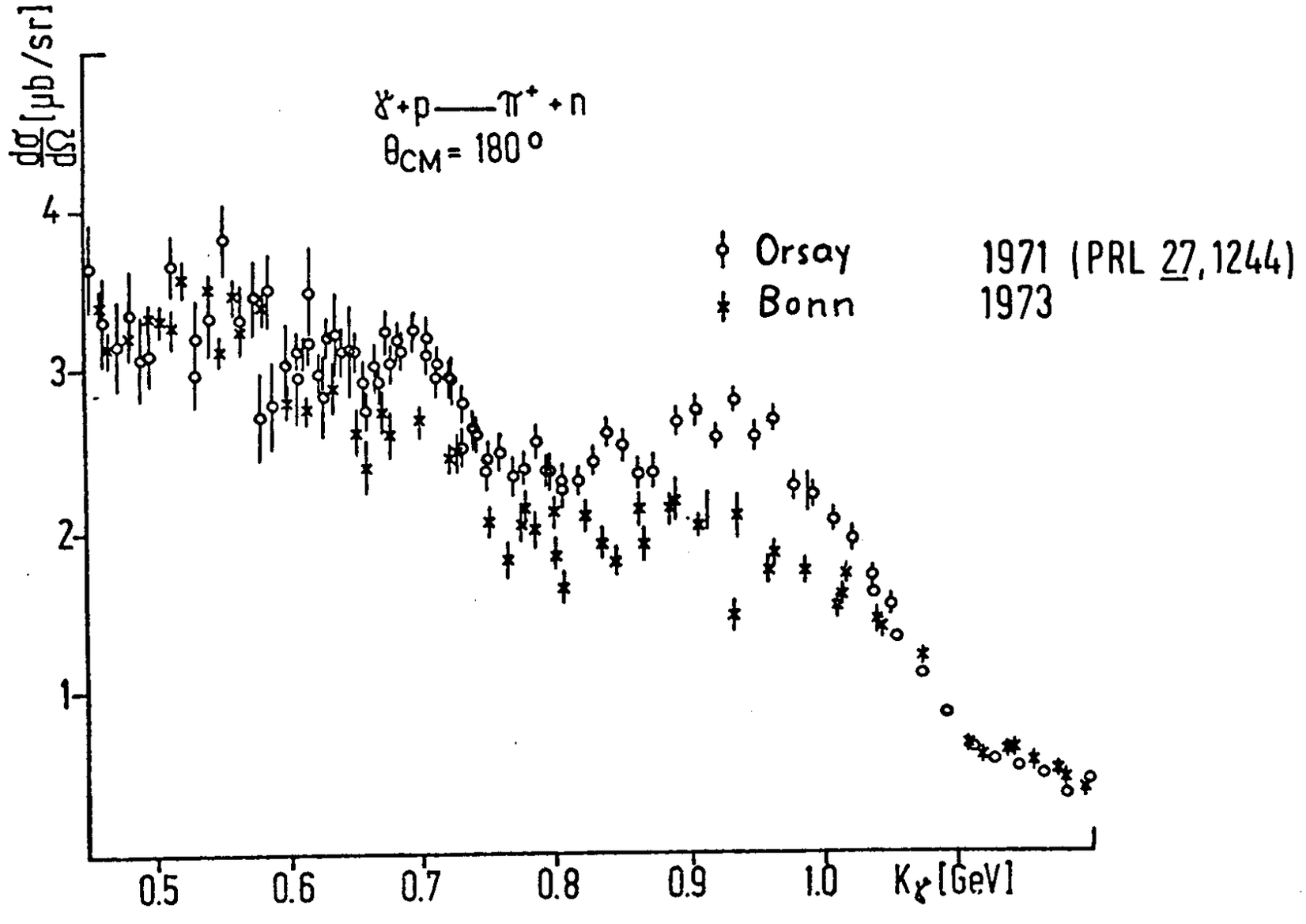
dσ/dΩ [μb/sr]
γ + p ——— π⁺ + n
θCM = 180°
Orsay 1971 (PRL 27, 1244)
Bonn 1973
4
3
2
1
0.5
0.6
0.7
0.8
0.9
1.0
Kγ [GeV]

Fig. 1

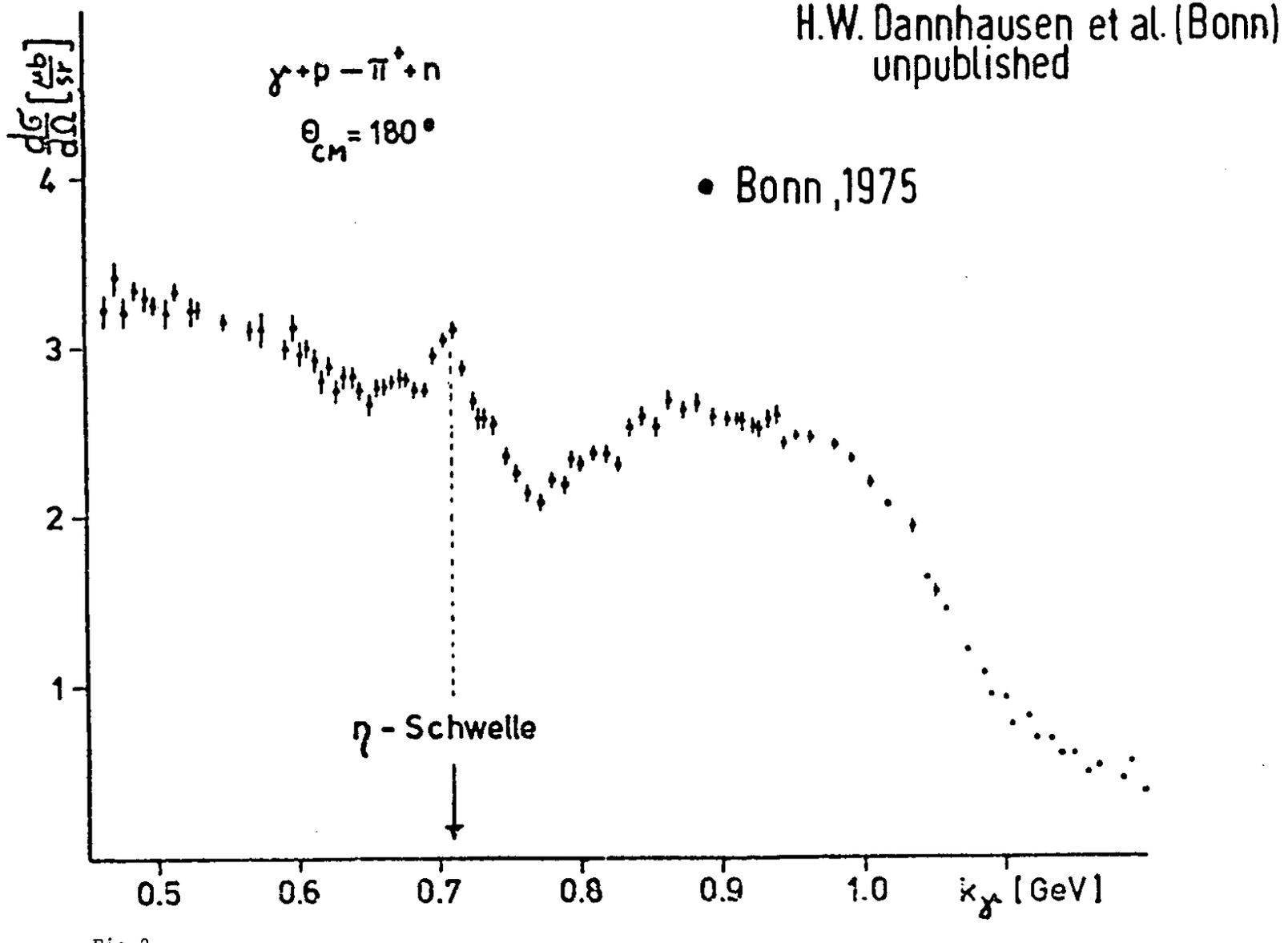
H.W. Dannhausen et al. (Bonn)
unpublished
$\gamma + p \to \pi^0 + n$
$\Theta_{CM} = 180°$
• Bonn, 1975
$\frac{d\sigma}{d\Omega}$ [$\frac{\mu b}{sr}$]
4
3
2
1
η - Schwelle
0.5
0.6
0.7
0.8
0.9
1.0
k_γ [GeV]

Fig.2

Final state	$\pi^+ n$				$\pi^0 p$				$\pi^- p$				σ
Exp. quantity	σ	P	Σ	T	σ	P	Σ	T	σ	P	Σ	T	σ
Data used by KMO (1973)	1614	12	91	24	1209	139	38	98	526	1	54	0	0
Berkeley (73/74)			42				48				45		
Kyoto (73)													42
Tokyo (74)				22				35					
NINA (74/75)		~26	~200	~100			~120	?					

Fig.3

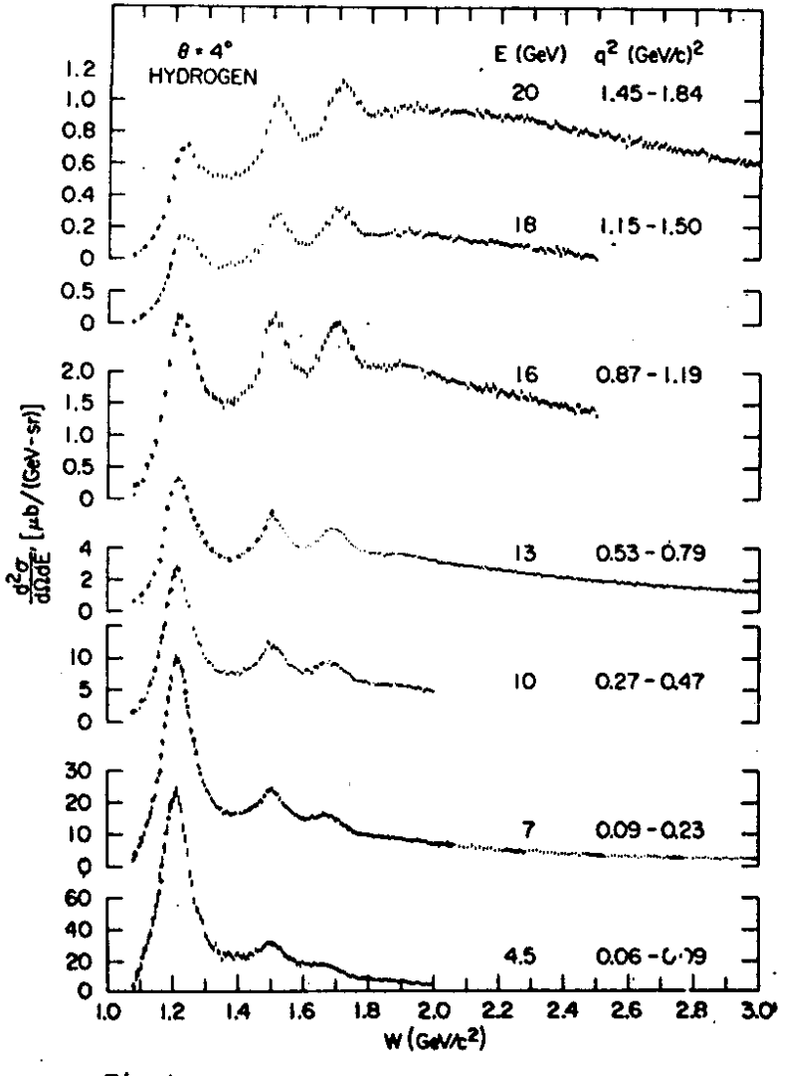
θ = 4°
HYDROGEN
E (GeV) q² (GeV/c)²
20 1.45 - 1.84
18 1.15 - 1.50
16 0.87 - 1.19
13 0.53 - 0.79
10 0.27 - 0.47
7 0.09 - 0.23
4.5 0.06 - 0.09
d²σ/dΩdE' [μb/(GeV-sr)]
W (GeV/c²)

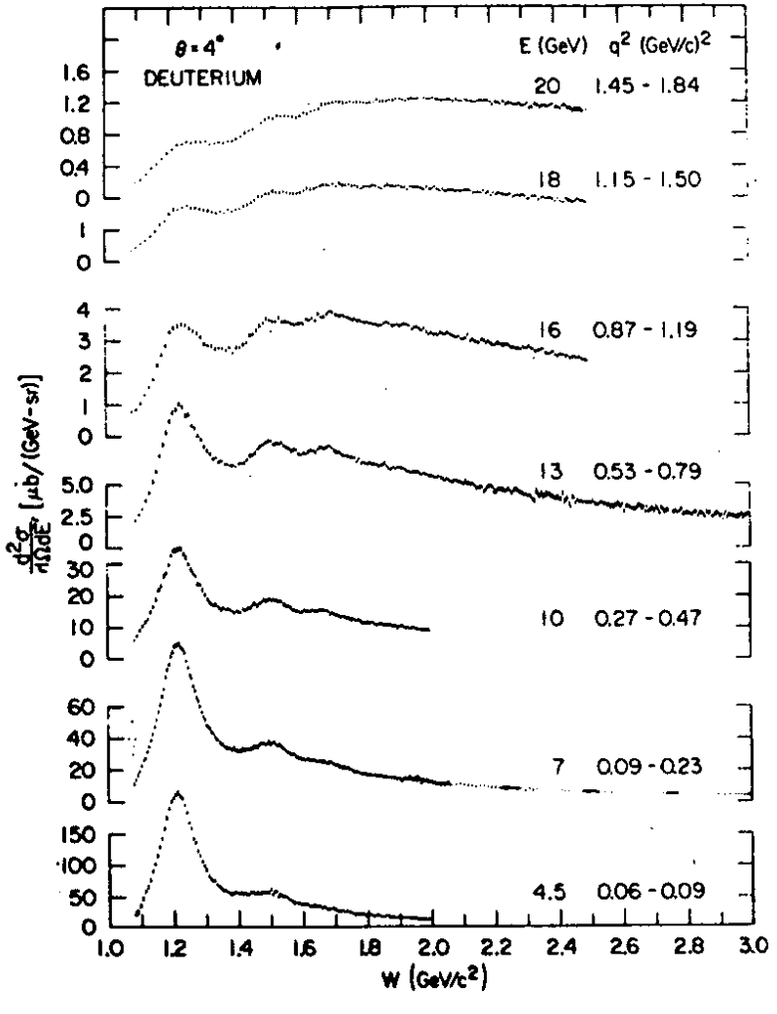
θ = 4°
DEUTERIUM
E (GeV) q² (GeV/c)²
20 1.45 - 1.84
18 1.15 - 1.50
16 0.87 - 1.19
13 0.53 - 0.79
10 0.27 - 0.47
7 0.09 - 0.23
4.5 0.06 - 0.09
d²σ/dΩdE' [μb/(GeV-sr)]
W (GeV/c²)

Fig.4

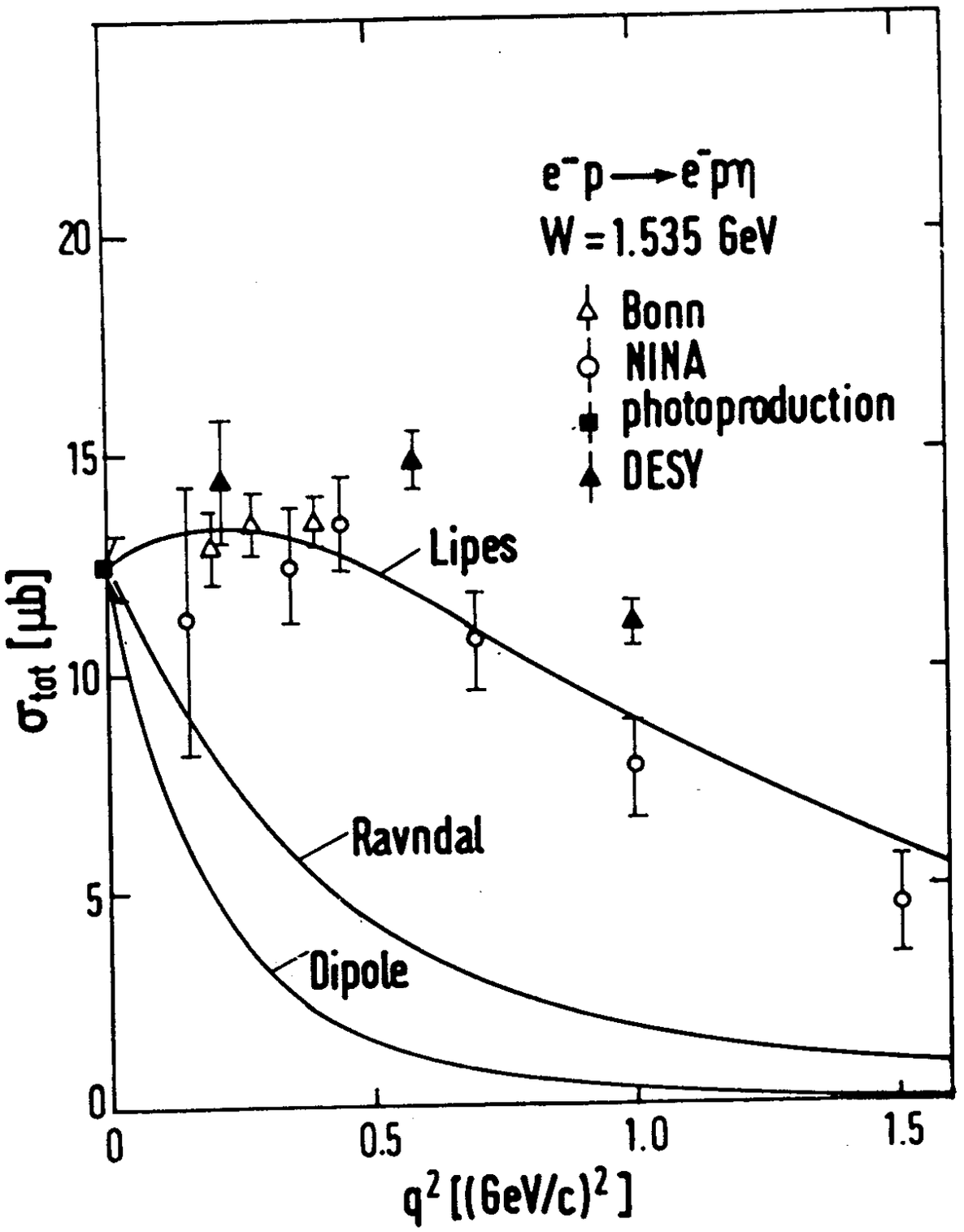
e⁻p → e⁻pη
W = 1.535 GeV
Bonn
NINA
photoproduction
DESY
Lipes
Ravndal
Dipole
σtot [μb]
q² [(GeV/c)²]
0
5
10
15
20
0
0.5
1.0
1.5

Fig.5

$$\gamma_v p \longrightarrow \pi^+ n$$

$W = 1175$ $\qquad$ $q^2 = 0.2\,(GeV/c)^2$

ε	E (MeV)	E'(MeV)	Θ_e	P_π (MeV/c)	Θ_π
0.20	357.1	69.7	77°3	242.9	11°3
0.65	522.0	234.7	32°7	242.9	21°3

$$\sigma_L = 5.7 \pm 1.7\ \mu b$$

$$\sigma_T = 11.3 \pm 3.0\ \mu b$$

$$R = \sigma_L / \sigma_T = 0.5 \pm 0.2$$

Fig.6

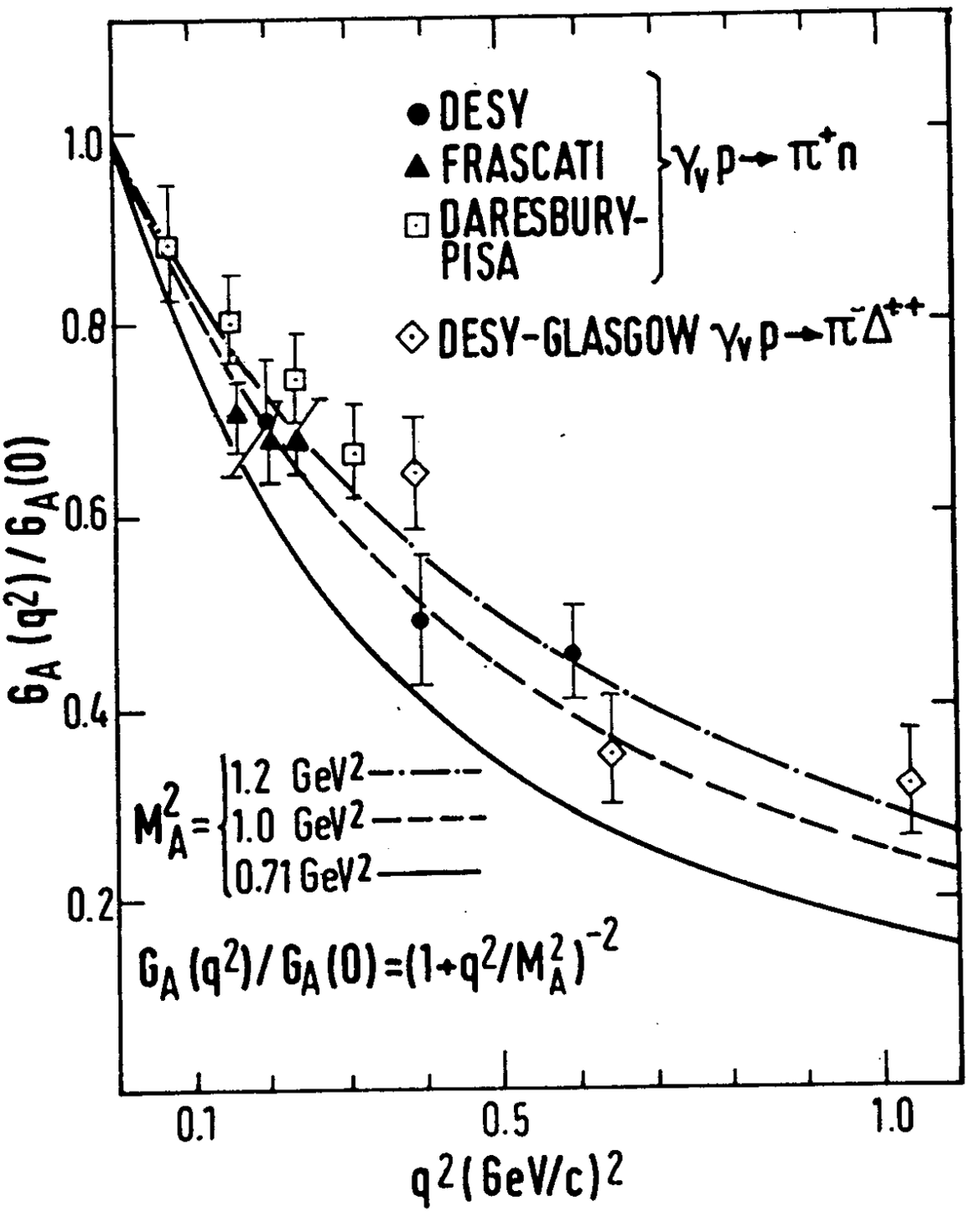
● DESY
▲ FRASCATI
⊡ DARESBURY-PISA
$\gamma_v p \to \pi^+ n$
◇ DESY-GLASGOW $\gamma_v p \to \pi^- \Delta^{++}$
$M_A^2 =$ 1.2 GeV²
1.0 GeV²
0.71 GeV²
$G_A(q^2)/G_A(0) = (1+q^2/M_A^2)^{-2}$
$G_A(q^2)/G_A(0)$
q^2 (GeV/c)²
1.0
0.8
0.6
0.4
0.2
0.1
0.5
1.0

Fig.7

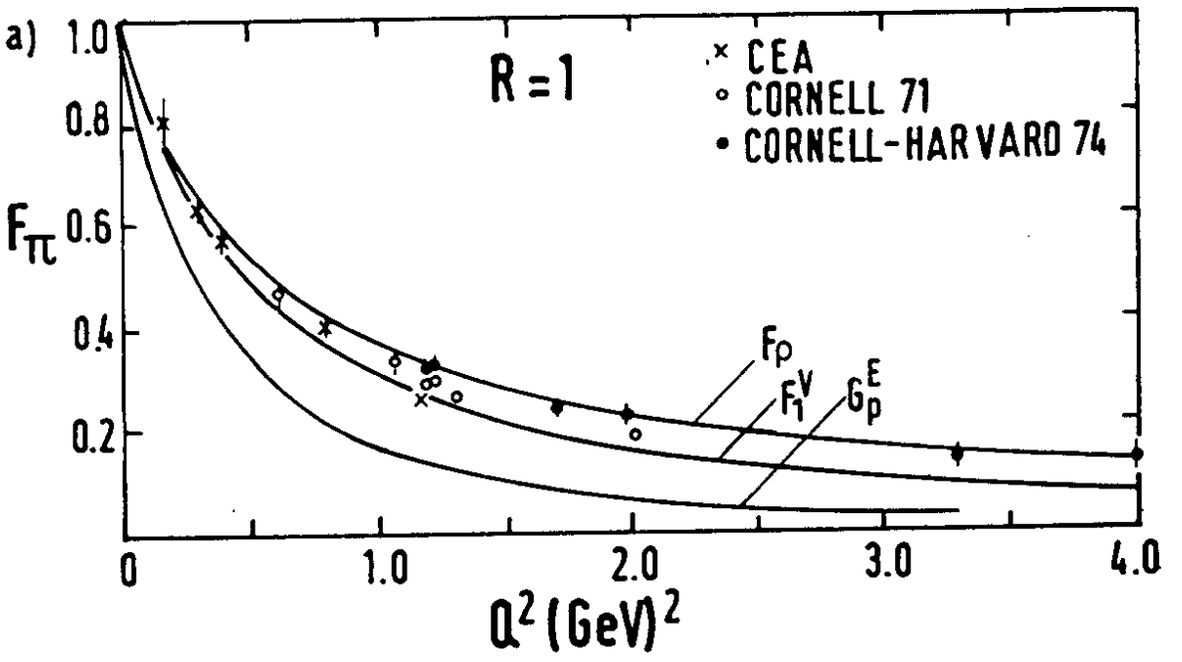
a)
R = 1
× CEA
∘ CORNELL 71
• CORNELL-HARVARD 74
F_{π}
F_p
F_1^V
G_p^E
Q^2 (GeV)^2

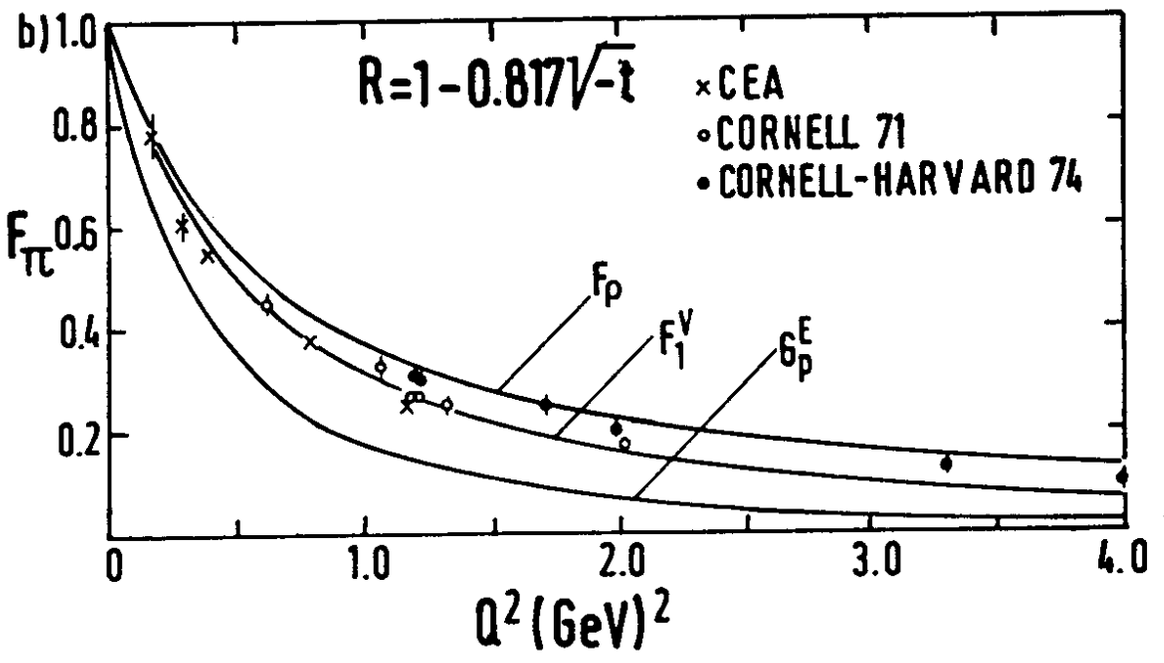
b)
$R = 1 - 0.817\sqrt{-t}$
×CEA
∘CORNELL 71
•CORNELL-HARVARD 74
F_{π}
F_p
F_1^V
G_p^E
Q^2 (GeV)^2

Fig.8

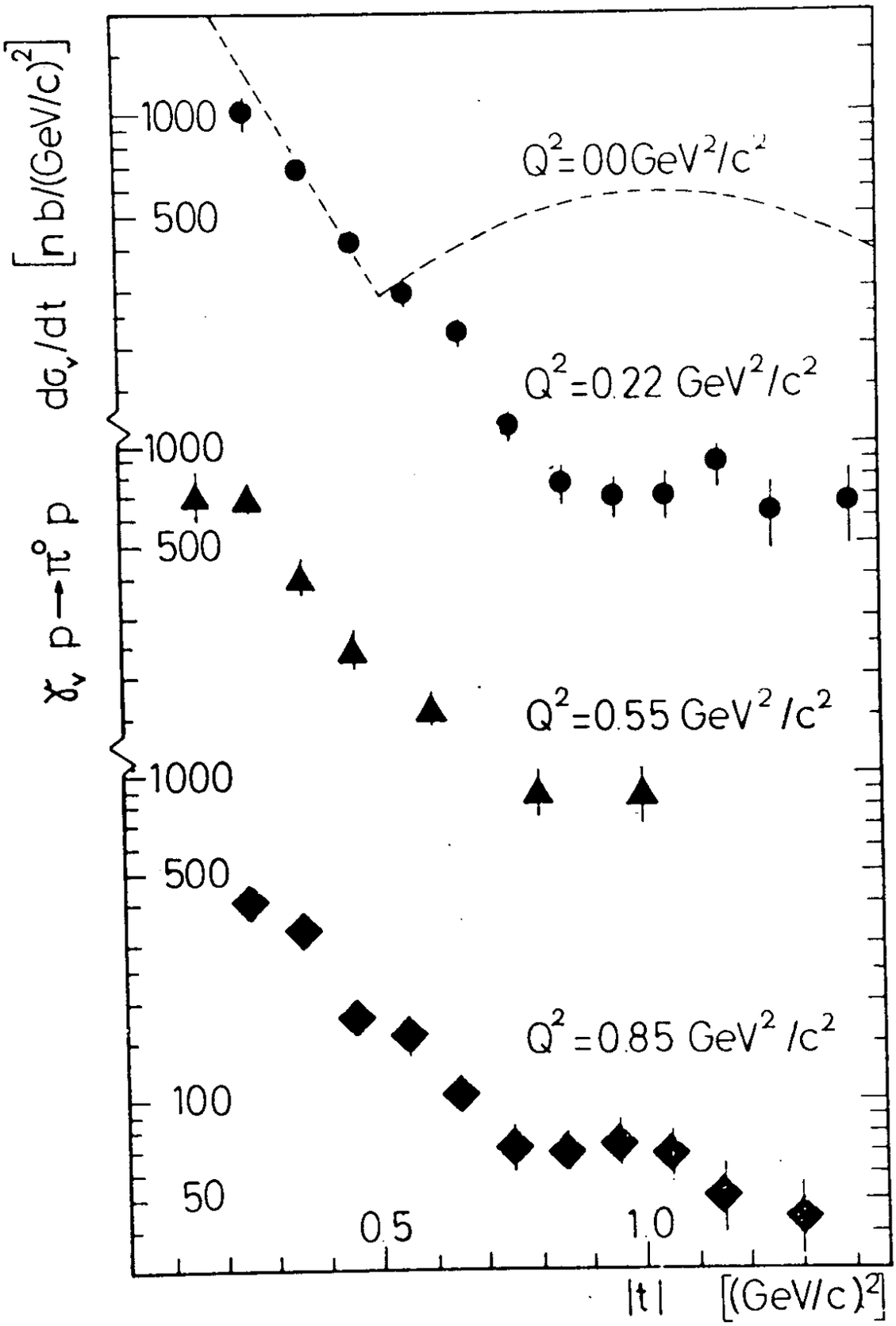
$\gamma_v p \to \pi^0 p$ $d\sigma_v/dt$ [nb/(GeV/c)^2]
1000
500
1000
500
1000
500
100
50
Q^2=00GeV^2/c^2
Q^2=0.22 GeV^2/c^2
Q^2=0.55 GeV^2/c^2
Q^2=0.85 GeV^2/c^2
0.5
1.0
|t| [(GeV/c)^2]

Fig.9

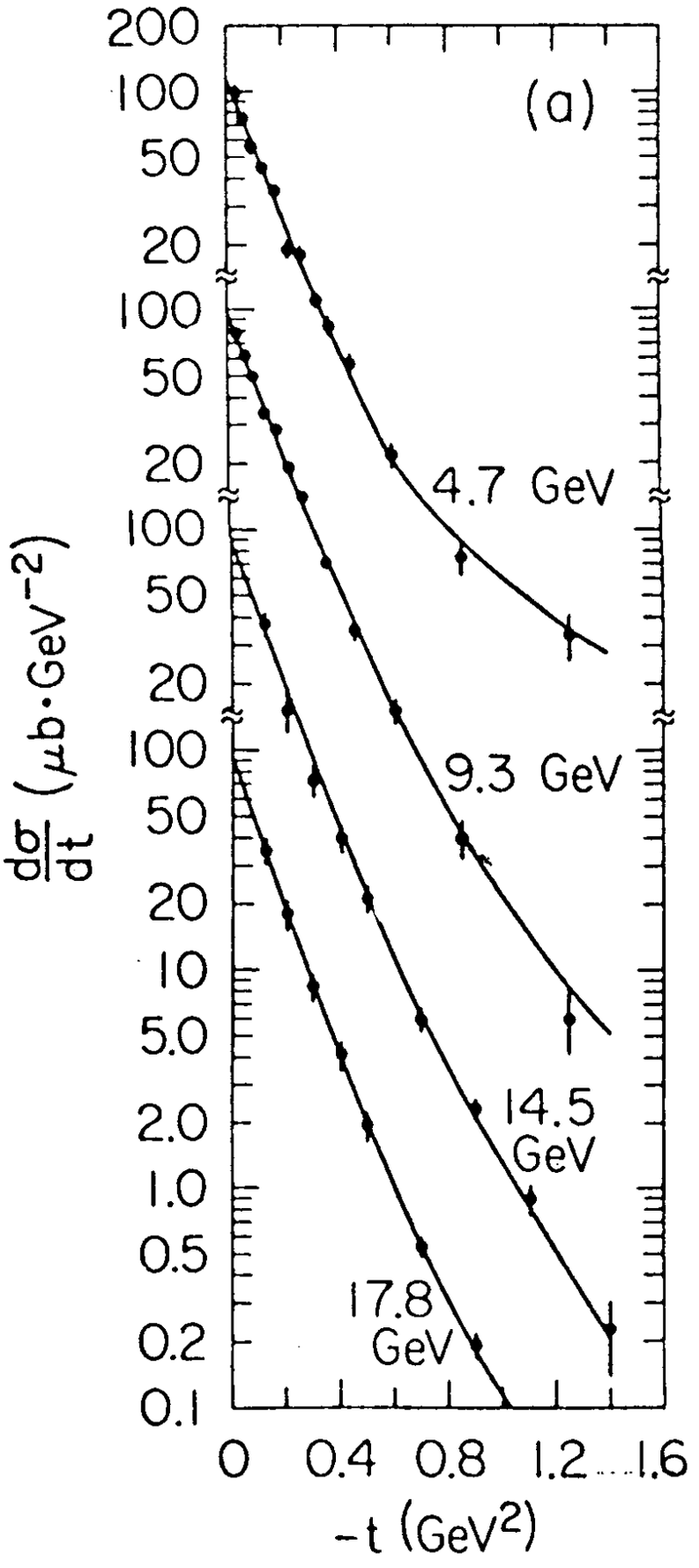
200
100
50
20
100
50
20
100
50
20
100
50
20
10
5.0
2.0
1.0
0.5
0.2
0.1
(a)
4.7 GeV
9.3 GeV
14.5 GeV
17.8 GeV
0
0.4
0.8
1.2
1.6
$\frac{d\sigma}{dt}$ (μb·GeV^{-2})
-t (GeV^2)

Fig. 10

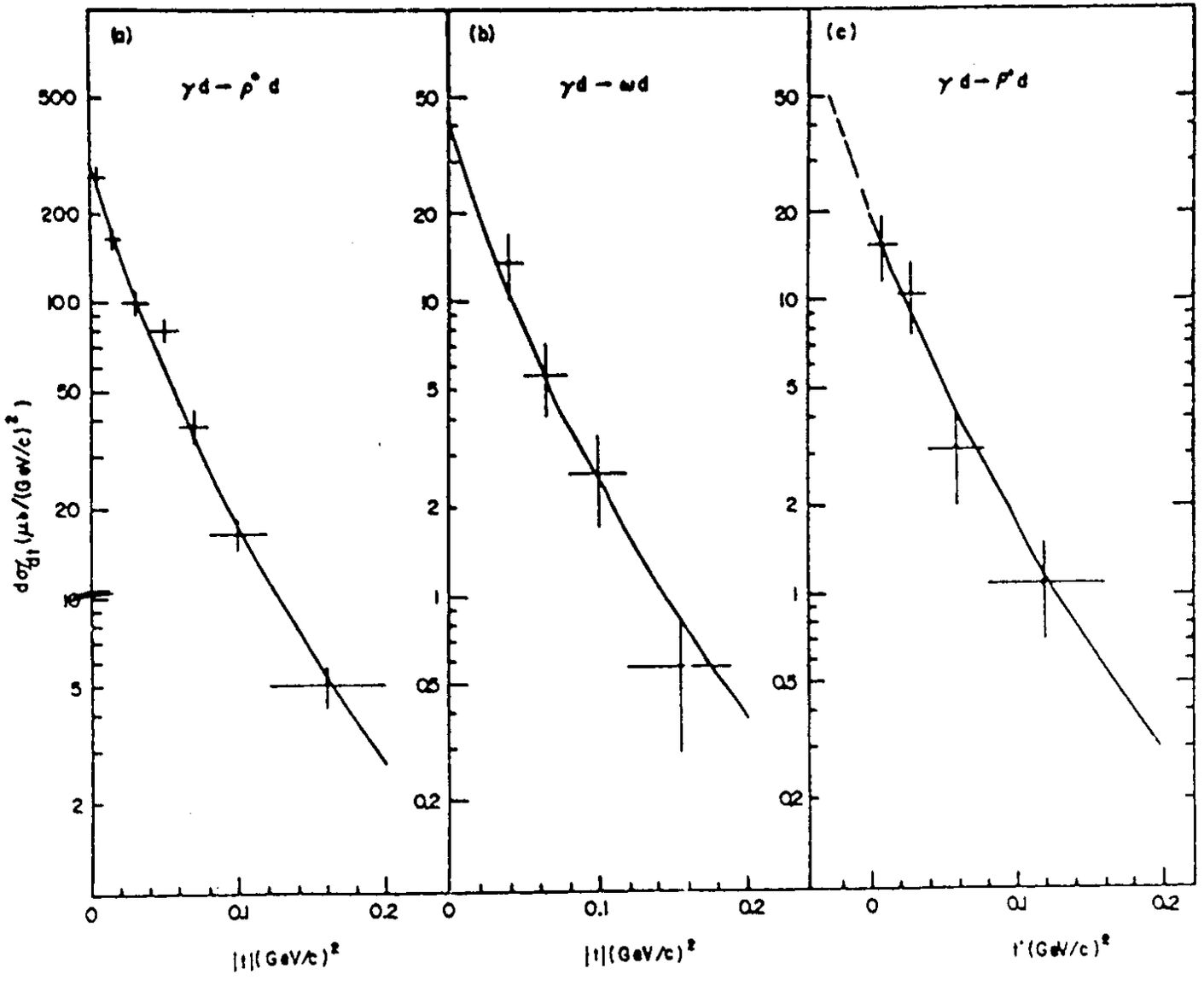

Fig.11

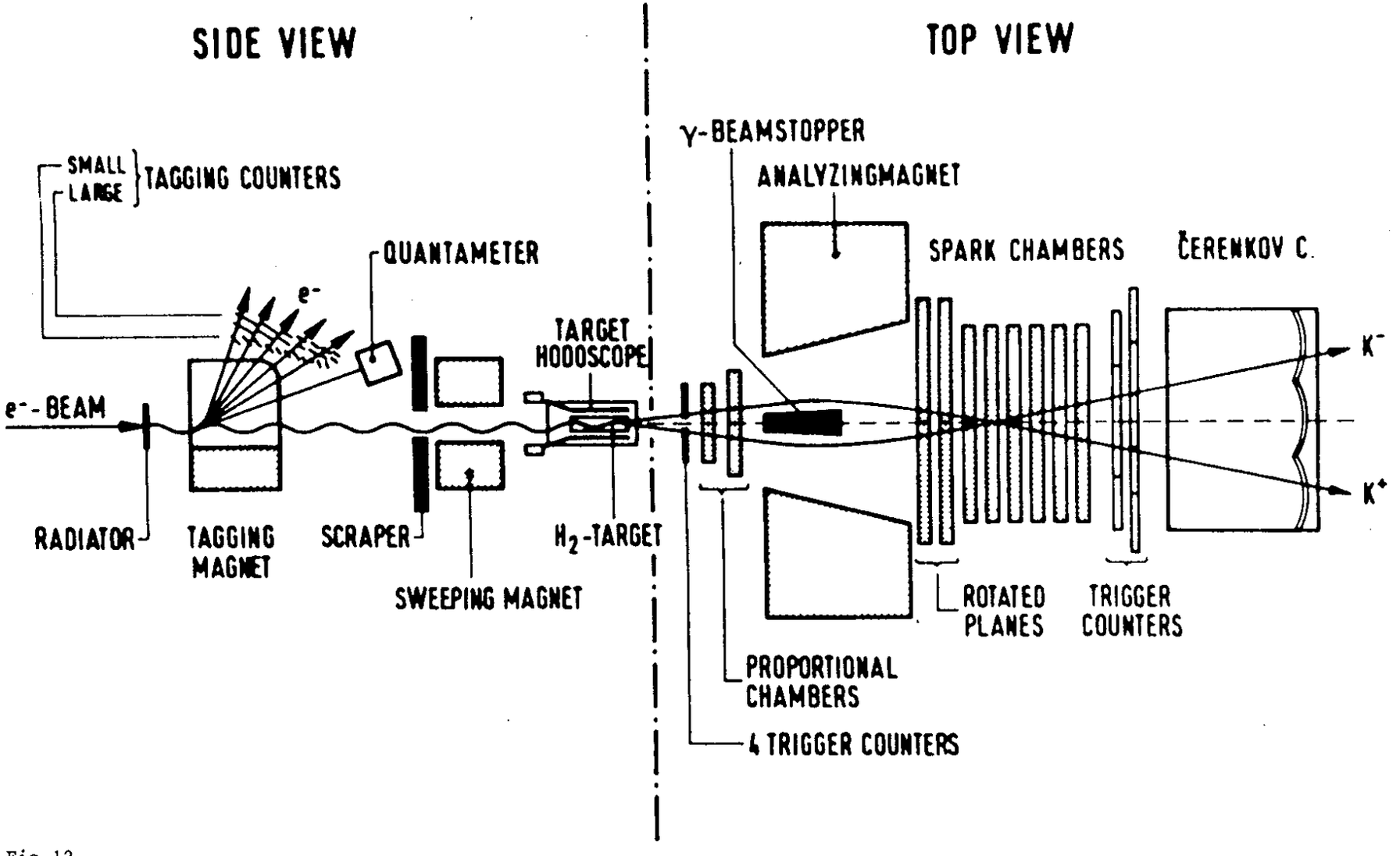
SIDE VIEW
TOP VIEW
SMALL
LARGE
TAGGING COUNTERS
QUANTAMETER
e⁻
e⁻-BEAM
RADIATOR
TAGGING MAGNET
SCRAPER
SWEEPING MAGNET
TARGET HODOSCOPE
H₂-TARGET
γ-BEAMSTOPPER
ANALYZINGMAGNET
SPARK CHAMBERS
ČERENKOV C.
K⁻
K⁺
ROTATED PLANES
TRIGGER COUNTERS
PROPORTIONAL CHAMBERS
4 TRIGGER COUNTERS

Fig.12

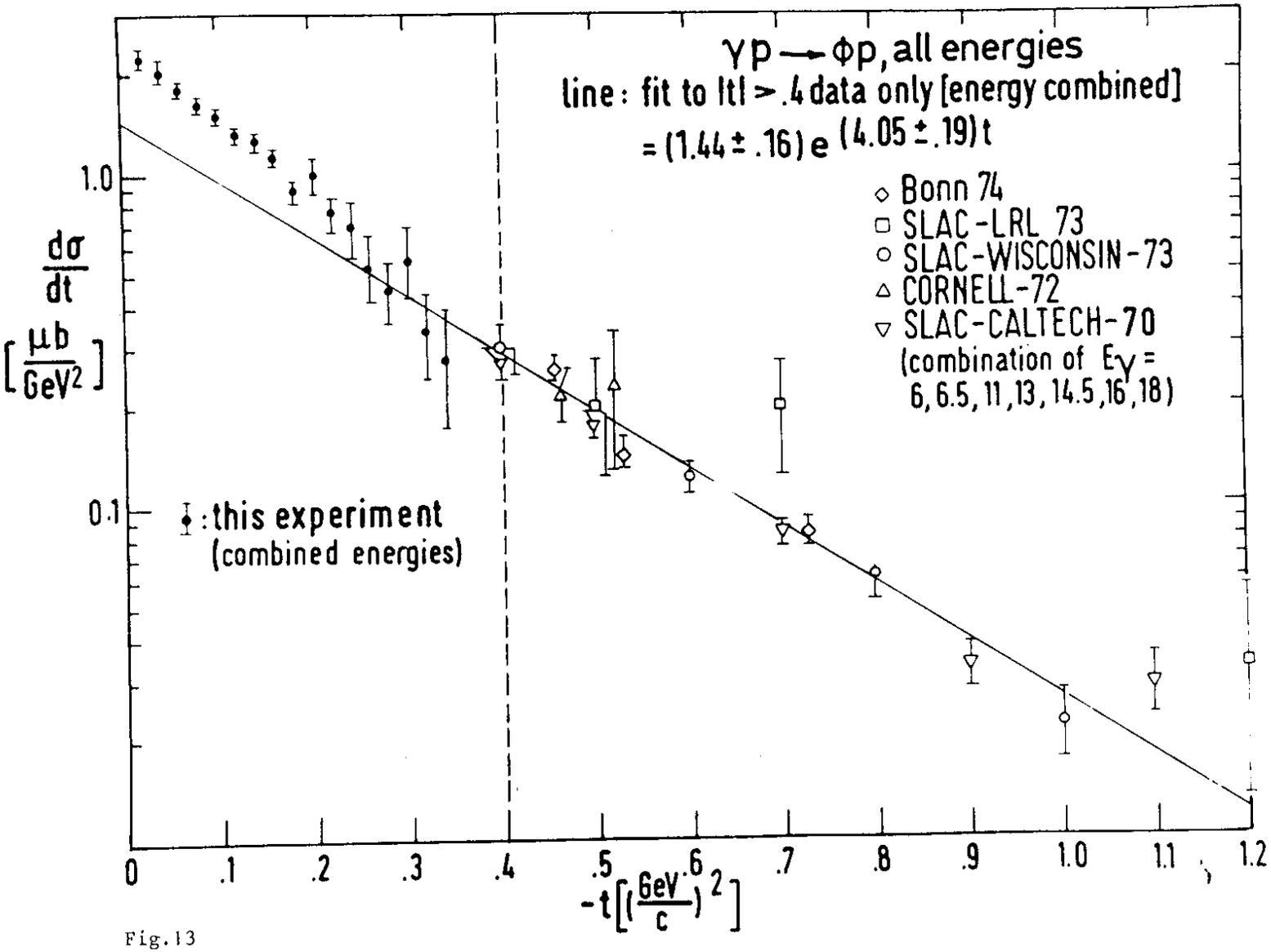
γp → φp, all energies
line: fit to |t| > .4 data only [energy combined]
= (1.44 ± .16) e (4.05 ± .19) t
◇ Bonn 74
□ SLAC-LRL 73
○ SLAC-WISCONSIN-73
△ CORNELL-72
▽ SLAC-CALTECH-70
(combination of Eγ = 6, 6.5, 11, 13, 14.5, 16, 18)
dσ/dt [μb/GeV²]
1.0
0.1
: this experiment
(combined energies)
0
.1
.2
.3
.4
.5
.6
.7
.8
.9
1.0
1.1
1.2
-t [(GeV/c)²]

Fig.13

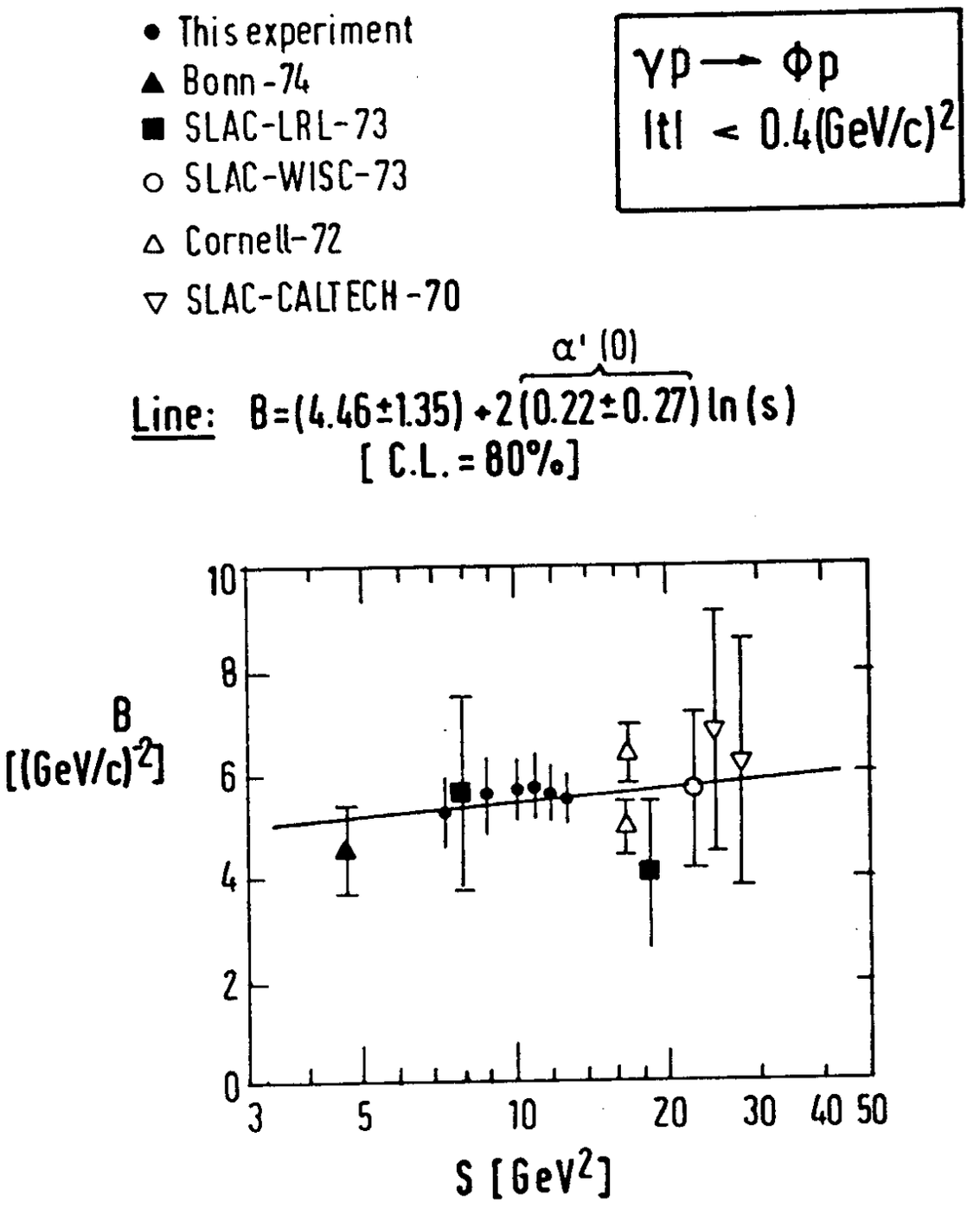
● This experiment
▲ Bonn-74
■ SLAC-LRL-73
○ SLAC-WISC-73
△ Cornell-72
▽ SLAC-CALTECH-70
γp → Φp
|t| < 0.4(GeV/c)²
α'(0)
Line: B=(4.46±1.35)+2(0.22±0.27) ln(s)
[C.L.=80%]
B [(GeV/c)⁻²]
10
8
6
4
2
0
3
5
10
20
30
40
50
S [GeV²]

Fig.14

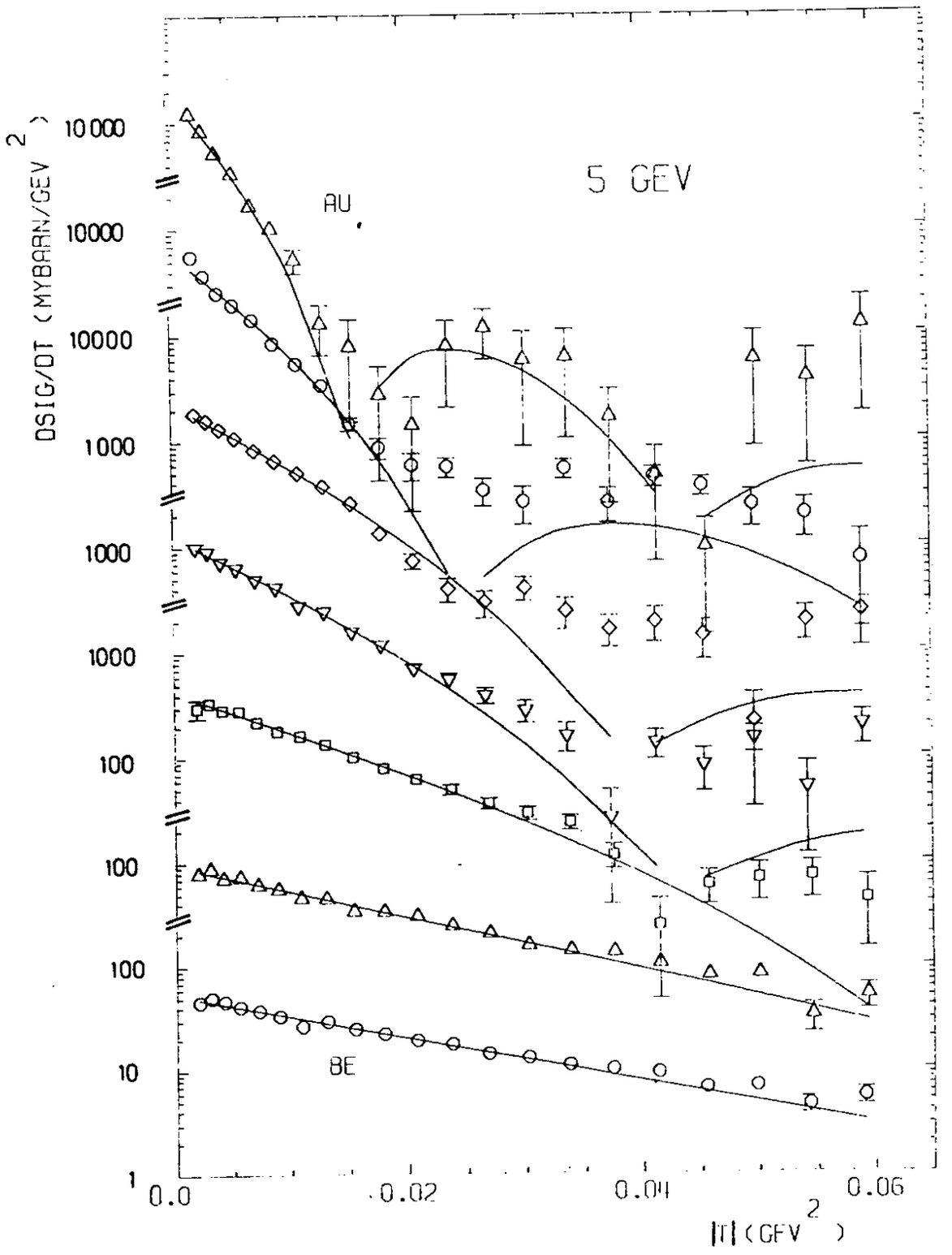
5 GEV
AU
BE
DSIG/DT (MYBARN/GEV 2)
10 000
10000
10000
1000
1000
1000
100
100
100
10
1
0.0
0.02
0.04
0.06
|T| (GEV 2)

Fig.15

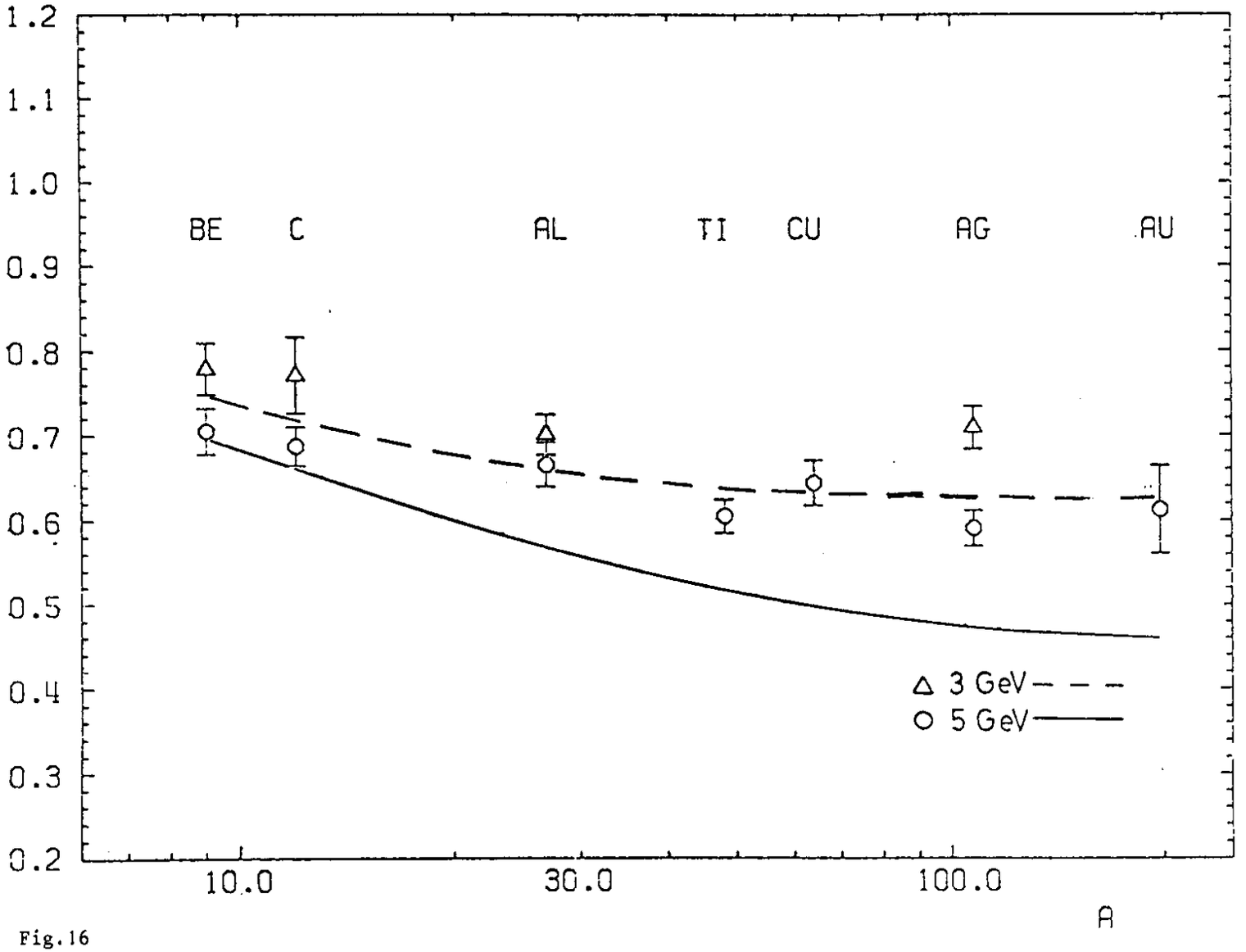
1.2
1.1
1.0
0.9
0.8
0.7
0.6
0.5
0.4
0.3
0.2
BE
C
AL
TI
CU
AG
AU
10.0
30.0
100.0
A
△ 3 GeV
○ 5 GeV

Fig.16

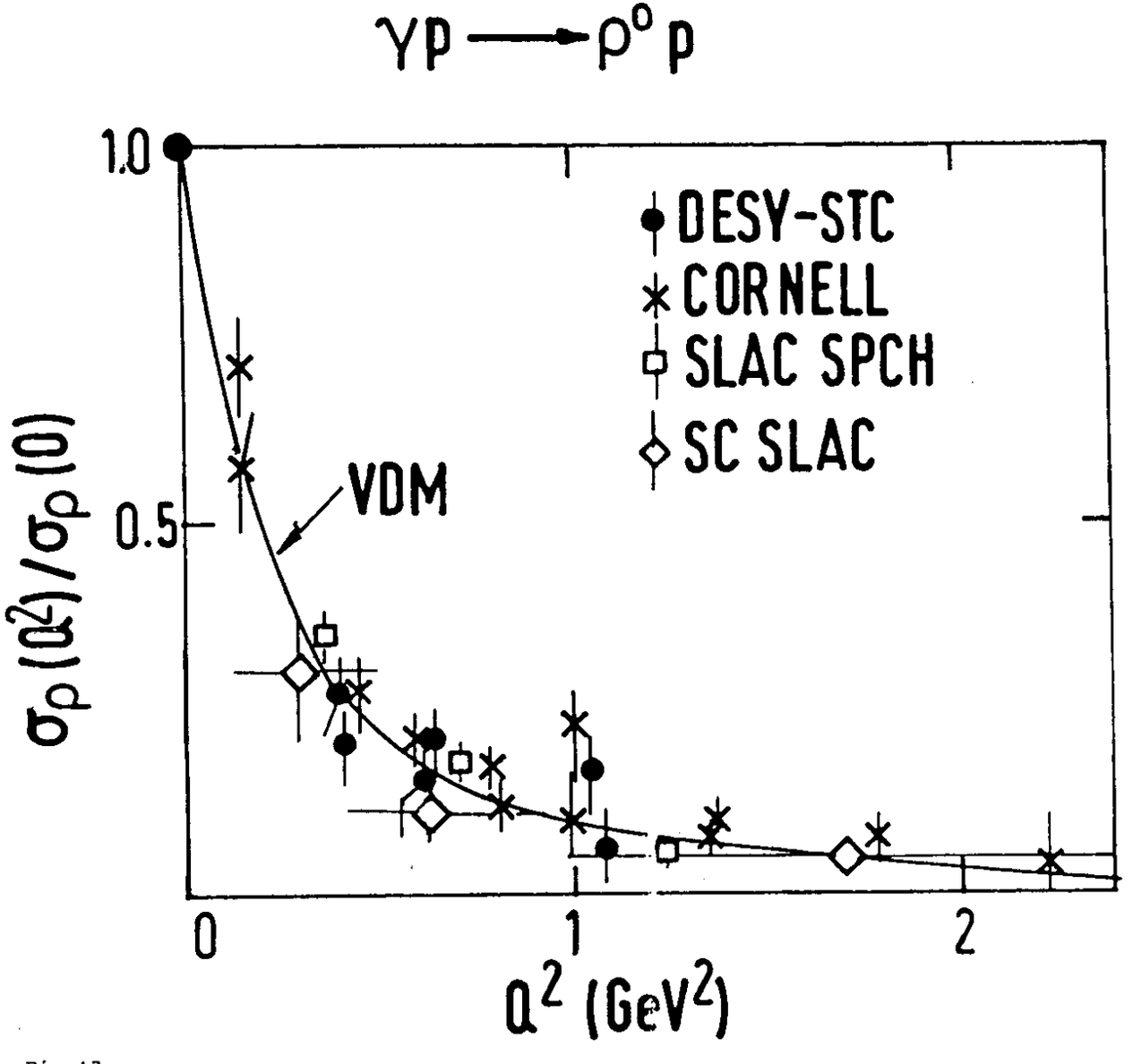
γp ⟶ ρ⁰ p
1.0
0.5
0
1
2
σρ(Q²)/σρ(0)
Q² (GeV²)
DESY-STC
CORNELL
SLAC SPCH
SC SLAC
VDM

Fig.17

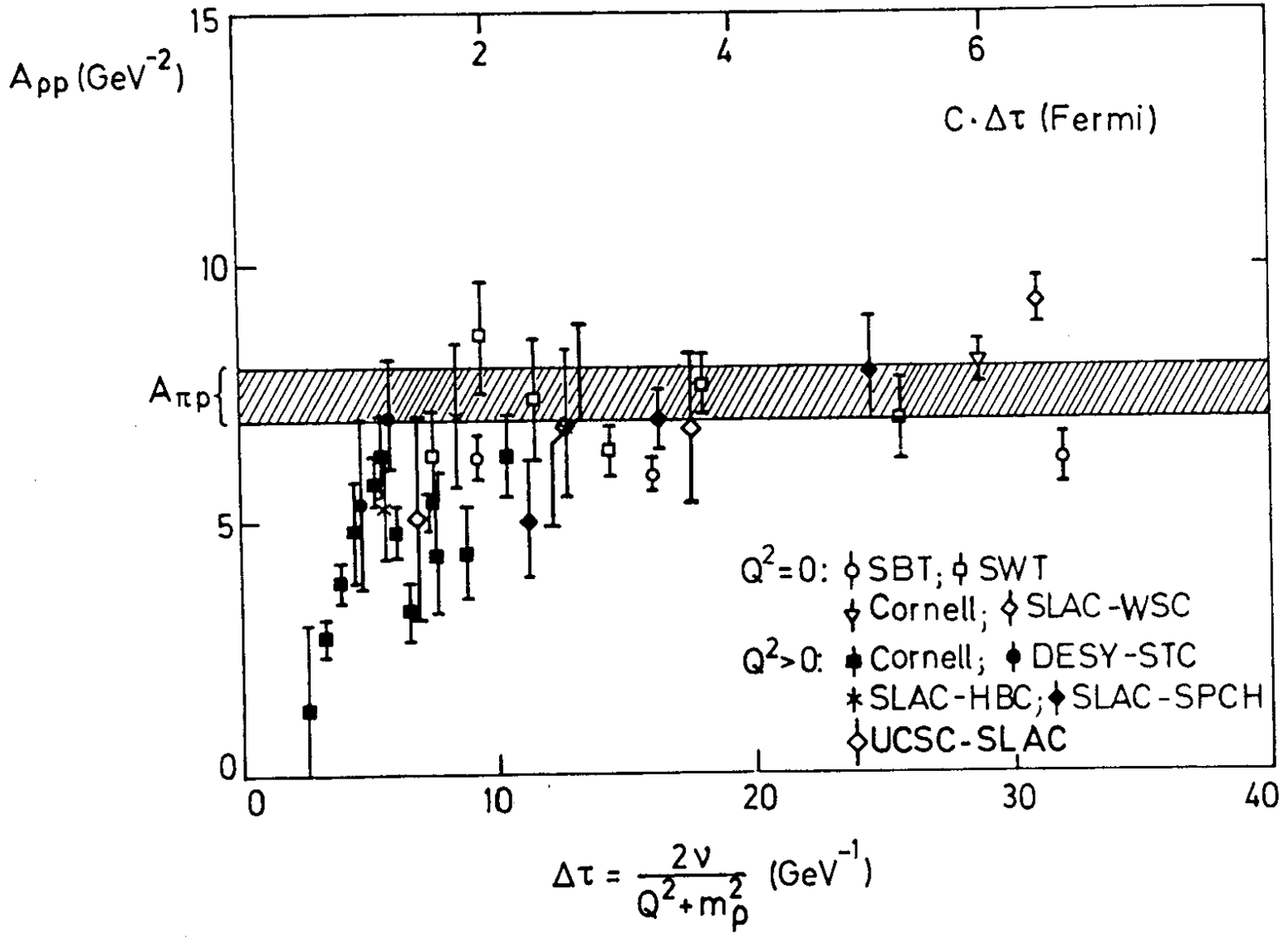
A_{pp} (GeV^{-2})
15
10
5
0
2
4
6
C·Δτ (Fermi)
$A_{\pi p}$
$Q^2=0$: SBT; SWT
Cornell; SLAC-WSC
$Q^2>0$: Cornell; DESY-STC
SLAC-HBC; SLAC-SPCH
UCSC-SLAC
0
10
20
30
40
$\Delta\tau = \frac{2\nu}{Q^2+m_\rho^2}$ (GeV^{-1})

Fig.18

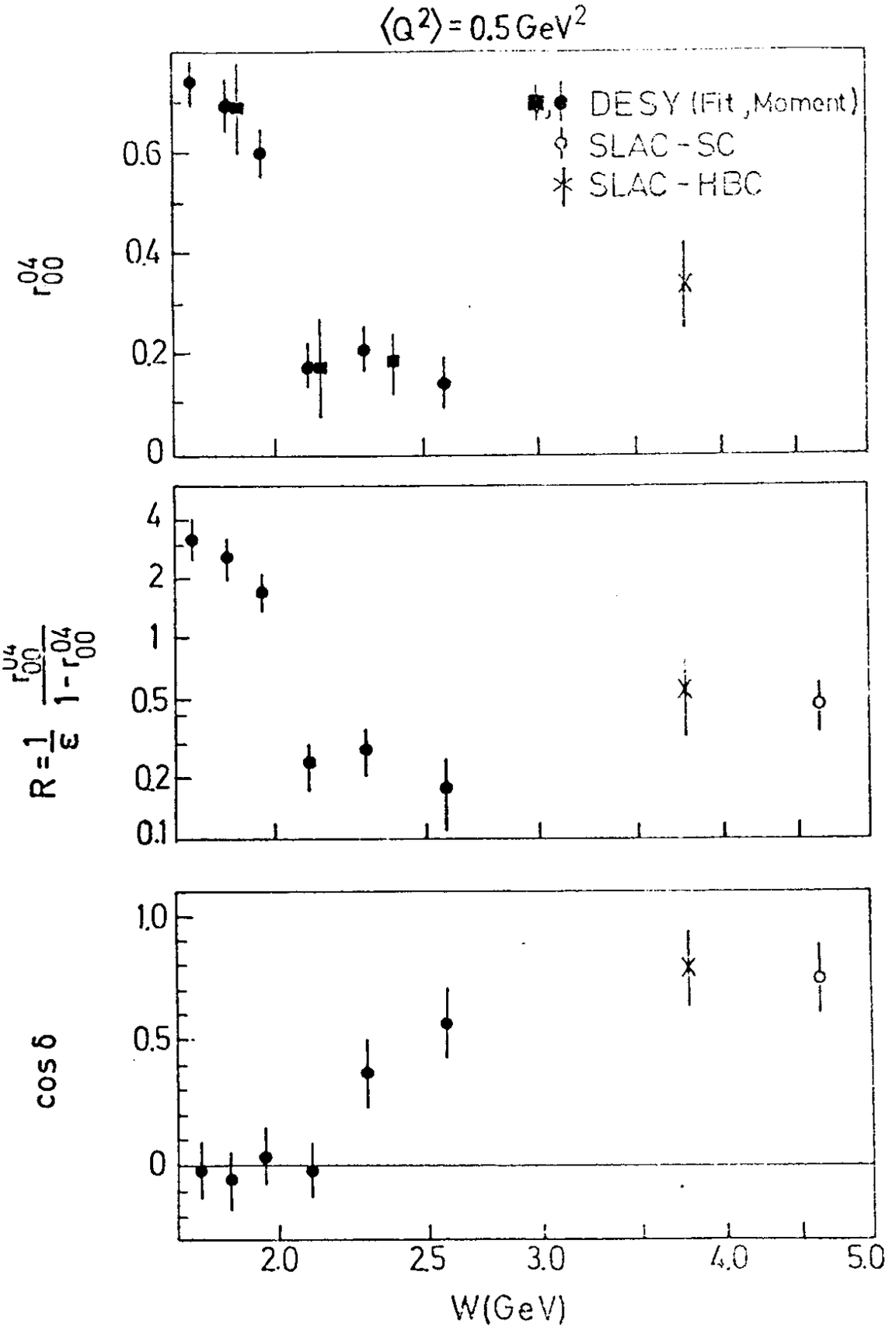
⟨Q²⟩ = 0.5 GeV²
DESY (Fit, Moment)
SLAC - SC
SLAC - HBC
r_{00}^{04}
$R = \frac{1}{\varepsilon}\frac{r_{00}^{04}}{1-r_{00}^{04}}$
cos δ
W(GeV)

Fig. 19

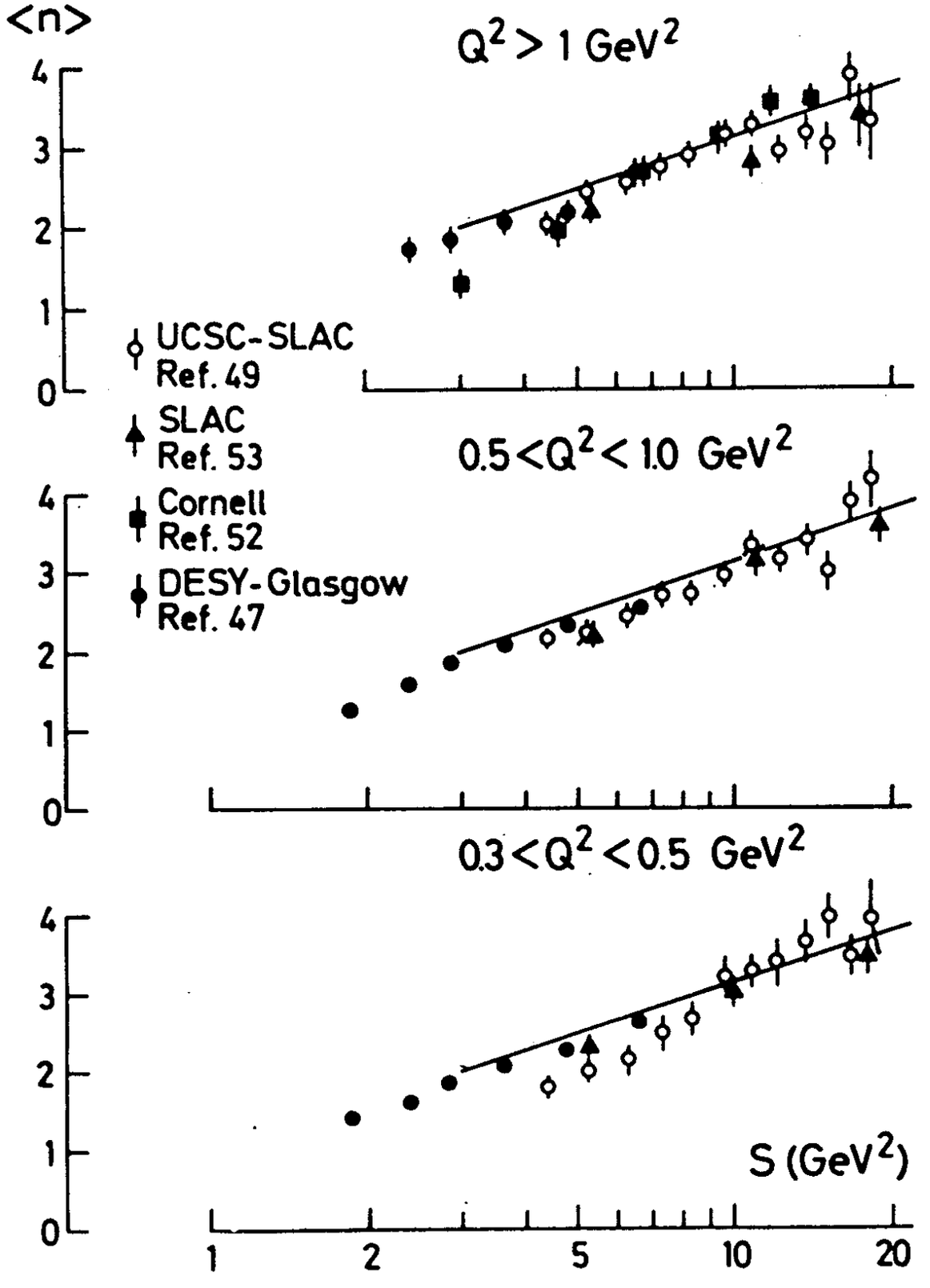
<n>
$Q^2 > 1$ GeV^2
UCSC-SLAC
Ref. 49
SLAC
Ref. 53
Cornell
Ref. 52
DESY-Glasgow
Ref. 47
$0.5 < Q^2 < 1.0$ GeV^2
$0.3 < Q^2 < 0.5$ GeV^2
S (GeV^2)
0
1
2
3
4
1
2
5
10
20

Fig.20

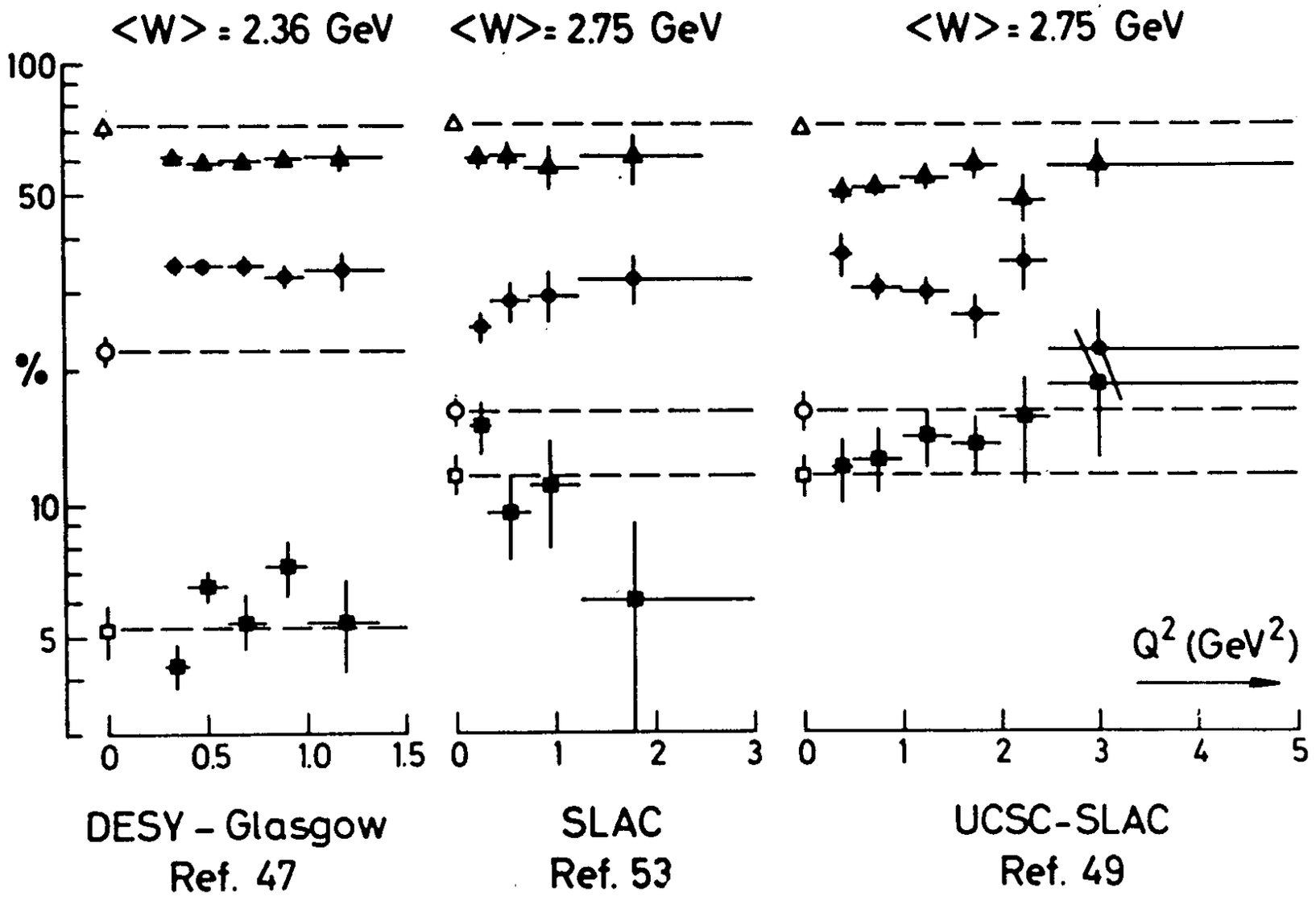
<W> = 2.36 GeV
<W>= 2.75 GeV
<W> = 2.75 GeV
100
50
%
10
5
0
0.5
1.0
1.5
0
1
2
3
0
1
2
3
4
5
Q² (GeV²)
DESY – Glasgow
Ref. 47
SLAC
Ref. 53
UCSC-SLAC
Ref. 49

Fig.21